THE EFFECT OF STRAIN RATE AND PLY GEOMETRY ON THE STRESS-STRAIN PROPERTIES OF NYLON YARNS

Frank Figucia, Jr.

Army Natick Laboratories
Natick, Massachusetts

September 1969

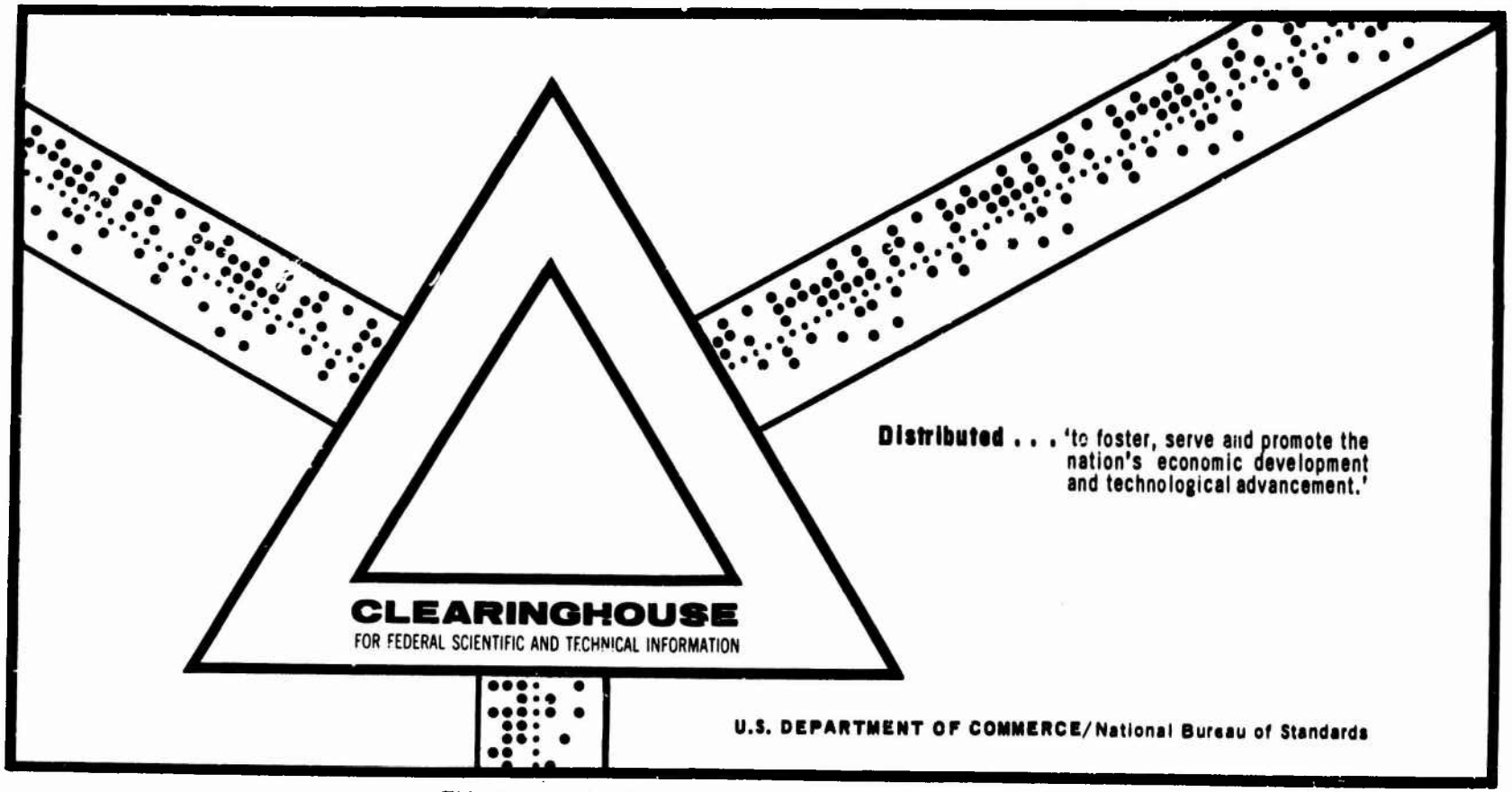

TECHNICAL REPORT

70-25-CE

THE EFFECT OF STRAIN RATE AND PLY GEOMETRY ON THE STRESS-STRAIN PROPERTIES OF NYLON YARNS

by

Frank Fasucio, Jr.

September 1967

UNITED STATES ARMY
NATICK LABORATORIES
Natick, Massachusetts 01760

Clothing and Personal Life Support Equipment Laboratory

TS-165

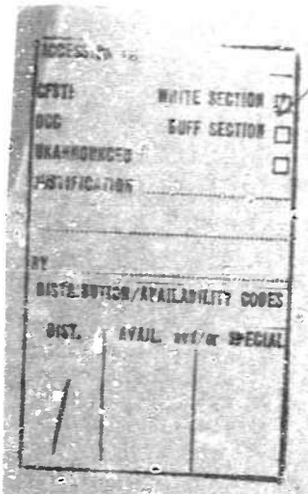

This document has been approved for public release and sale; its distribution is unlimited.

Citation of trade names in this report does not constitute an official indorsement or approval of the use of such items.

Destroy this report when no longer needed. Do not return it to the originator.

AD_____

TECHNICAL REPORT

70-25-CE

THE EFFECT OF STRAIN RATE AND PLY GEOMETRY ON THE STRESS-STRAIN PROPERTIES OF NYLON YARNS

by

Frank Figucia, Jr.
Fiber and Fabric Research and Engineering Branch
Textile Research and Engineering Division

Project Reference:
1T024401A329

Series: TS-165

September 1969

Clothing and Personal Life Support Equipment Laboratory
U.S. ARMY NATICK LABORATORIES
Natick, Massachusetts 01760

FOREWORD

This report presents a comparison of the stress-strain behavior of nylon yarns at a conventional (slow) rate of tensile strain to that at a very rapid rate. The rapid rate is a simulation of the actual strain applied during airdrop operations.

The data developed contribute to a broader research program designed to characterize material behavior under more realistic laboratory test conditions. This portion of the work was accomplished under Project Number 1T024401A329, Organic Materials Research for Army Materiel.

Differences noted in yarn behavior at the two strain rates used here, as well as differences noted in previous work on braided cord, emphasize the potential for improvement in the control of system design and safety factors. Airdrop system components, previously designed on the basis of performance under quasi-static loading conditions, may in the future be re-evaluated in terms of more realistic information such as is being developed under this program. This re-evaluation would undoubtedly lead to cost savings through improvement in design efficiency.

The author is indebted to members of the staff at the Lowell Technological Institute, where analyses of yarn geometry were conducted. The support of Professor John J. McDonald, Head of the Department of Textile Technology, and the advice of Professors David H. Pfister and Fritz F. Kobayashi were greatly appreciated. Special acknowledgment is also extended to Mr. Louis I. Weiner and Mr. Leo McCafferty of the Fiber and Fabric Research and Engineering Branch, U. S. Army Natick Laboratories for their assistance and advice.

CONTENTS

CONTENTS (cont'd)

LIST OF TABLES

LIST OF TABLES (cont'd)

LIST OF FIGURES

LIST OF FIGURES (cont'd)

ABSTRACT

The purpose of this study was to examine the changes that take place in the stress-strain behavior of plied yarns due to the differences in straining rates, and also the effects that yarn geometry has on these changes.

A series of 12 nylon plied yarns, representing a gradual build-up in geometric complexity, was examined. Ply structure was varied by twisting two, three, five and seven strands to various levels. A single untwisted strand was also used to provide reference data representative of yarn with relatively little translational complexity. Yarns were identified in terms of their ply torsion. This parameter, which provides a numerical description of the geometric orientation of the ply components, is calculated from their helix angle, diameter and retraction.

Tensile strength, elongation and work-to-break were measured for all samples at strain rates of 100 and 288,000 %/min. These properties were then compared to geometric torsional levels, thus relating trends in physical yield to changes in structural complexity. They were also compared to the single strand reference data, providing an analysis of translational efficiency trends with structural changes.

Results showed that the capability to translate forces and energy through these yarns decreases with increases in geometric complexity under the impact loading condition. At standard quasi-static loading rates, however, strength translation remains fairly stable and energy translation increases with structure. Then the relative trends are diverging at the two test speeds. The use of low-speed data in the design of items for high strain rate use provides an overestimation of the actual end-use performance.

Mathematical expressions were derived from which impact performance can be predicted from known information at conventional test speeds.

THE EFFECT OF STRAIN RATE AND PLY GEOMETRY ON THE STRESS-STRAIN PROPERTIES OF NYLON YARNS

1. Introduction

The stresses and strains applied externally to textile items during their normal use are the object of much concern to the textile engineer. In many cases, the final design of a textile end-item is based primarily upon these basic mechanical considerations. However, the rate of speed at which these stresses and strains are imposed, although recognized as a significant factor, has not been sufficiently dealt with, particularly in items such as auto seat belts, parachutes, climbing ropes, and tire cords where the applied rate of strain is extremely high. It is likely that maximum efficiency and durability are not being attained due to insufficient information on the behavior of fibers and structures under these extreme conditions.

Data have been developed and published describing the behavior of single fibers and single-ply, low-twist yarns subjected to tensile loading at very rapid strain rates. Much less work has been done on the higher forms of yarn structure, the more complex braided and woven structures, and splices (stitched seams and knots).

To introduce and define the areas of investigation being considered in this present study, some basic trends noted in previous investigations on a braided structure are first presented.

A single strand of continuous filament nylon yarn at a very low level of twist exhibited the following ultimate properties when tested to rupture at a high strain rate:

1. Breaking strength greater than at low strain rate
2. Ultimate elongation less than at low strain rate
3. Work-to-break approximately equal to that at low strain rate.

The strain rates were 100%/min (low) and 238,000%/min (high).

When continuous filament nylon yarns were highly twisted, plied and combined into a tightly braided structure, the following properties were noted at high strain rates:

1. Breaking strength less than at low strain rate
2. Ultimate elongation less than at low strain rate
3. Work-to-break approximately one half that at low strain rate.

The significant differences in comparing the yarn behavior to the braid behavior are as follows:

1. Instead of showing greater strength at the high strain rate, in the braid form the yarns lose strength at the high rate.

2. The high strain rate strength decrease of the braid coupled with its decrease in ultimate elongation results in a decrease in work-to-break. This combined effect is important in materials undergoing shock-type loadings in which total energy absorption is a major factor.

The above example illustrates the tendency of materials to deteriorate in performance with increases in structural complexity. The differences in strength and energy outputs noted for the single yarn and the braid represent extremes in behavior which reflect extremes in structure.

The general approach taken in this study was to define the translational responses of structures which lie between the extremes considered above. This was done by beginning with the single untwisted yarn and building through systematic ply and twist combinations to a seven-ply, nine tpi structure. The general purpose is to present an analysis of the high-speed performance of these yarns.

2. Literature Survey

a. Yarn Geometry

The geometry of plied structures has not been as extensively treated as has the geometry of single strand structures. However, the literature is not devoid of presentations in this area, and sufficient theory is available to describe parameters pertinent to this study.

Woods[1], using strings as models, considered the twist geometry of yarns back in 1933. He originated the term "tortuosity" which has since been used extensively. He noted that the twist in a component of a plied yarn is related to the inclination of the helical path which it follows, and offered a mathematical expression for tortuosity.

Schwarz[2], in analyzing ply helix geometry, gave a detailed derivation of the tortuosity expression, and Treloar[3], predicting stress-strain behavior, used similar relationships. Treloar also used an expression for total yarn torsion which has been adopted for this study.

Treloar's predictions were checked experimentally by Riding[4] who also presented data obtained for ply axis radius and ply retraction of two, three, and sevenfold Tenasco cords.

Tattersall[5] also presented experimental results for single yarn retraction and helix angle which he compared to some earlier predictions of Treloar[6].

b. High-Speed Test Instruments

A variety of test instruments have been devised through the years for the tensile testing of textile materials at high strain rates.

Leaderman[7], Schwarz[8], Newman[9], and others used gravity methods, in which a freely falling weight was guided so that it dropped onto a plate supported by a test specimen - to rupture the specimen through the impact. Results could be obtained electronically or by calculation from known input energies.

Parker and Kemic[10], Ballou and Roething[11], Lang[12] and others have also used the gravity principle by swinging the weight on a pivoted pendulum. This allowed for transverse or tensile application of the load depending upon the clamping system used. The falling pendulum instruments were more limited in velocity potential compared to the free-falling weight instruments.

"Rotating disk" testers were developed and used by Meredith[13], McCrackin et al.[14], and others. With these instruments power was

obtained through a rapidly rotating disc which engaged a fixture holding one end of the sample (head end) and propelled it forward. Photographic techniques were used to trace the relative distance travelled by the head mass and another known mass attached to the tail of the sample. From this information, distance-time and velocity-time curves could be plotted from which peak stresses and strains could be derived.

Numerous ballistic methods of test have been reported in which a missile is projected against a specimen, loading it transversely. One particularly impressive instrument was described by Chu, Coskren and Morgan[15]. This device develops rupture forces up to 200,000 pounds at striking velocities of 800 ft/sec. Projectiles as heavy as 10 pounds may be used.

Pneumatically driven testers, such as the FRITS Instrument described in this report, have been used relatively recently. An instrument which may be powered either pneumatically or hydraulically is described by Supnick and Silberberg[16] as having a capacity of 10,000 pounds at a maximum velocity of approximately 14 ft/sec.

c. Plied Yarn Tests at High Speed

Studies have been made on natural and synthetic yarns at high strain rates, using the various test instruments described above. In general, rupture strength is greater at high strain rate than at conventional, and ultimate elongation is less. These trends have been reported for nylon yarns by Smith[17], Meredith[13] and Smith et al.,[18] who used falling weight, rotating disc and transverse methods, respectively.

Lyons and Prettyman[19] reported another interesting effect concerning energy absorption. In analyzing tirecord made from various fibers, they showed that the high/low strain rate energy ratio was lowest for nylon compared with the other fibers tested.

3. Experimental Procedure

a. Geometric Properties

The yarn series investigated in this study consisted of 13 yarns of various ply and twist combinations designed to represent a systematic build-up of structural complexity which would form a logical basis for comparing behavioral trends in stress-strain response. The final structures were processed through the Lowell Technological Institute

Research Foundation. All plied yarns were formed from the same lot of nylon 66 single yarn obtained from the E. I. duPont deNemours and Company. The singles were 210 denier, 34 filament made from duPont's type 330. The processed series investigated was as follows:

Ply	Twist (tpi)	Twist Direction
1	0.75	Z
2	2	Z
2	5	Z
2	9	Z
3	2	Z
3	5	Z
3	9	Z
5	2	Z
5	5	Z
5	9	Z
7	2	Z
7	5	Z
7	9	Z

Five ply levels were studied at three basic twist levels. Effective interpretation of the stress-strain behavior of these various structures required a system of geometric identification which could be applied at all levels and would provide a uniform terminology by which the structures might be compared.

The geometric parameter used was ply torsion as presented by L. R. G. Treloar[3]. Definitions of torsion and tortuosity are found in Appendix A. Ply torsion (ψ_o) is defined mathematically by the following relationship:

$$\psi_o = \psi_s \frac{l_s}{l_o} + \frac{1}{a_o} \sin\alpha \cos\alpha \qquad (1)$$

where:

ψ_o = ply torsion
ψ_s = single yarn torsion
l_s = yarn length/unit filament length for single yarn
l_o = ply length/unit single yarn length
a_o = ply axis radius
α = ply helix angle

To compute the ply torsion (ψ_o) it was necessary to obtain values for the various parameters of equation (1) applicable to each structure. This was done by laboratory evaluation for the ply helix angles (α), yarn length/unit filament length (l_s), and ply length/unit single yarn length (l_o). The ply axis radius (a_o) and the torsion in the singles yarn were obtained by appropriate calculation.

Each term of equation (1) will now be discussed.

(1) Single Yarn Torsion (ψ'_s). A plied yarn displays certain performance characteristics because of its structure as a bundle unit. That is to say that any one strand removed from the plied yarn will most likely not behave as the group of strands does. There is, however, a certain degree of influence exerted on the overall ply performance by the configuration of the single strands.

Equation (1) for total ply torsion includes the factor ψ'_s which represents the torsion of the individual component strands. Treloar defines this single strand torsion as:

$$\psi_s = 2\pi n_s \qquad (2)$$

where n_s simply represents the ply twist. It must be noted here that Treloar discusses plied yarns made up of zero-twist single strand components. Equation (2) is, therefore, valid since the individual components undergo a number of rotations equivalent to the turns applied to the total ply system, and the tpi in any individual strand is considered equal to the ply twist, neglecting small differences in total length of ply axis and single yarn axis.

Application of equation (2) to the yarns used in this study requires some adjustment, however, since the basic component yarn being used is a 0.75 tpi "Z" rather than a zero twist yarn. For example, if a group of these singles were combined with five turns of "Z" twist per inch, each strand would have acquired 5 tpi "Z", but the total twist in each would be 5.75 tpi "Z". Therefore, for this study, single yarn torsion (ψ_s) is computed as:

$$\psi_s = 2\pi(n_s + .75) \qquad (3)$$

where: n_s = ply twist (tpi)

Ply Twist (n_s)	Total Single Yarn Twist	Single Yarn Torsion (Ψ_s)
2	2.75 Z	17.28
5	5.75 Z	36.18
9	9.75 Z	61.30

(2) Single Yarn Retraction (l_s). When a group of yarn plies or a single ply bundle of filaments is twisted, a uniform unit is formed in which the component yarns or filaments spiral around an imaginary axis through the center of the unit. As more and more twist is added, the length of the newly formed single or plied yarn becomes shorter and shorter. The commonly used term for this shortening is yarn retraction.

Retraction cannot be ignored as a factor in this study. For example, a 3-ply yarn, fully twisted to 5 tpi has a total length (L). Removal of the five turns of ply twist would produce three strands of length (l_1), which is longer than "L". Further removal of twist from the three individual strands would result in zero - twist bundles of filaments of length (l_2), longer still than "L".

The overall ply Torsion (Ψ_o), as presented in equation (1), takes into account retraction effects through the use of the terms l_s and l_o. The yarn length per unit filament length of the individual plies is expressed as l_s. As the three plies of yarn are twisted about the imaginary ply axis, each strand is also undergoing twist about its own axis. If one of these plies of length l_1 were removed and untwisted to length l_2, then the ratio of l_1/l_2 would yield the required retraction (l_s) for the single strand component of the yarn structure. Determination of the l_s values in the laboratory would then seemingly require such a removal of the individual plies from the fully twisted structure. This could not be accomplished with accuracy, so an alternate method was employed.

Single ply yarn from the same lot used for this study was placed in a Suter Twist Tester and the producer's twist removed. This zero - twist reference length was recorded, as read directly from the Suter scale. Twist was then introduced and the yarn strand was allowed to retract freely under the influence of the added twist. A total of approximately 250-260 turns were applied and twist readings taken at every 0.05 inches of retraction. The twist per inch could then be read and the "l_s" value computed for every point at which readings were taken. Five runs were made on separate yarn samples and the "l_s" values plotted against tpi

values for all five runs. "l_s" values for all of the yarn structures under investigation can be obtained by entering the graph at the twist level to which the single yarns were actually configured in the final structure.

The laboratory data obtained by the above procedure are tabulated in Appendix B, Table IV.

(3) Ply Yarn Retraction (l_o). As was mentioned in the discussion of single ply retraction, when a group of three individual yarn strands is formed into a single plied yarn by twisting, the length (L) of the plied unit continually shortens with the addition of twist. The ratio of this length of the total ply structure (L) to the helical length (l_1) of one of its three components is what has been defined as ply yarn retraction (l_o).

Determination of the change in length due to the plying operation was a routine laboratory process, again performed using the Suter Twist Tester. A known length (20 in.) of yarn was placed in the tester with care taken so that no twist was lost in handling. The sample was then untwisted to the zero level, being allowed to extend freely under the applied tension of the Suter apparatus (40 grams). The increase in length due to untwisting was then recorded directly from the Suter scale. The ratio of twisted to untwisted lengths could then be computed to provide "l_o" values for the 12 plied yarn structures. Three samples of each yarn were tested and the average l_o values for each yarn plotted.

The raw data obtained are recorded in Appendix B, Table V.

(4) Ply Helix Angle (α). Formation of a plied yarn may be defined as a permanent orientation of a number of single yarns into helical configurations about an imaginary ply axis. There are an infinite number of helical paths which may be followed by the ply component yarns about the ply axis. Although all the component strands follow individual spiral paths through space, they all tend to be parallel and form the same angle with the ply axis. So a convenient method of describing the helical aspects of the plied structure is to identify it by this helix angle.

Measurement of helix angle for the yarns in this study were made in the laboratory by microscopic techniques. A Bausch & Lomb instrument of the telescoping tube type was used, measuring at a total magnification of 116x.

Yarn packages were mounted horizontally on a metal rod attached to a laboratory ring stand from which the yarn was drawn into the field of view with care being taken to maintain the original twist while unwinding the yarn. The yarn was drawn across rollers on the microscope table and a tail was made to hang over the edge, to which was clipped an 11.1 gram weight. A measurement was made with the yarn under this tension. Ten determinations were made on each of the plied yarn samples with a minimum distance between successive measurements of approximately two feet.

Some inconsistencies in the helix angles at successive points along the yarn were noted, particularly in the low-twist yarns. This inherent condition and the difficulty involved in consistently estimating the imaginary ply axis were the main contributors to moderate within-sample variation. This was not considered to be significant, however, and the data obtained appear to be logical and acceptable.

Raw data with statistical analysis are recorded in Appendix B, Table VI.

(5) Ply Radius (a_y). The final geometric parameter required in determining ply yarn torsion by the method of Treloar is the radius of each ply structure in its final configuration. This can be readily obtained from yarn diameter data which are more common and can be developed in a number of ways.

It was decided that since the previously measured helix angles appeared to be consistent and reliable, a method of calculation based upon a theory which relates yarn diameter to helix angle would be valid.

The basic relationship considered, as presented by Schwarz[20], is as follows:

$$\tan \theta = d_y t \qquad (4)$$

where: θ = helix angle
d_y = total outer diameter
t = turns of ply twist per inch

Schwarz also differentiates between effective diameter (d_h) and outer diameter (d_y) and theorizes that the total diameter (d_y) of a plied structure does not influence the behavioral characteristics of the structure as much as the interstrand contact. He, therefore, establishes correction factors for plied yarn diameters based on the number of strands in the ply and the probable geometric orientation when these strands are combined. The above relationship then becomes:

$$\tan \theta = K d_y t \qquad (5)$$

where: K = Schwarz's correction factor
= 0.50 for 2 ply yarn
= 0.54 for 3 ply yarn
= 0.63 for 5 ply yarn
= 0.67 for 7 ply yarn
$Kd_y = d_h$ = effective diameter

Solving equation (4) for d_y and multiplying by the appropriate constant for each ply level yields the effective ply diameter (d_h). Taking one half of this value gives the required ply axis radius (a). Raw data are recorded in Appendix B, Table VII.

(6) Ply Torsion (Ψ_o). All the geometric parameters required to solve equation (1) for ply torsion (Ψ_o) have now been obtained. The values for each parameter at every level of yarn structure are summarized in Appendix B, Table VIII, with the calculated ply torsion for each structure also listed.

The ply torsion values represent a numerical description of the structural complexity of each yarn under study. As has been shown, these values represent the combined effects of single strand torsion, single strand and ply retraction, ply radius and ply helix angle. This provides a fairly comprehensive geometric description in one term which can be used to show the relative complexity of the various yarn structures in stress-strain analyses to follow.

b. Stress-Strain Tests

The objective of this study was to examine strain behavior of the yarn series at a conventional test rate and also at a very rapid rate. This examination was done at the U.S. Army Natick Laboratories through the use of two test instruments, the Instron Tensile

Tester and the FRITS Tester. Both provided permanent load-elongation traces from which ultimate rupture data could be obtained, or curves in terms of specific stress could be plotted.

The following sections provide more detailed descriptions of the test equipment and the methods employed in performing these tests.

(1) Low Strain Rate. Test Apparatus. An Instron Tensile Tester, Floor Model TTD was used to provide rupture strength and elongation, work-to-break and stress-strain data at the low strain rate. The instrument conditions were as follows:

Load Cell	CT
Jaw Speed (in/min)	5
Chart Speed (in/min)	10
Gage Length (in)	5
Jaws	Flat (1" x 3")

The gage length and jaws used were chosen mainly to conform with those necessitated by the design of the FRITS Tester, used for the high strain rate tests. As a result, complete conformity to standard ASTM or Military Test Methods was not maintained. It is not felt, however, that these variances had any adverse effect on the results obtained.

The Instron provides permanent representative traces of each test on a continuous paper roll chart. From these charts all the required data could be obtained for the analysis of the yarns at low strain rate. From the above test conditions, it is seen that this rate was 100%/min as the extension speed of 5 in/min was applied to a 5-inch specimen length.

Breaking Strength. Since each sample being tested represented a particular level of geometric complexity, it was essential that all tests be performed with the yarns at the prescribed level of twist. This required constant care in handling of the samples.

For the breaking strength tests, the yarn spool was mounted on a horizontal rod at the base of the Instron. The free end, which had been taped to the spool, was withdrawn and a sufficient length unwound so that no yarn was tested which could have been mishandled in previous tests and subsequently attached to the spool at a lower twist level.

Five specimens of each of the 13 yarn samples were tested.

Breaking strength values were easily obtained from the Instron chart records by proper interpretation of the horizontal displacement of the curve in terms of the calibrated full-scale displacement. Yarn strengths of approximately 2-25 pounds were encountered in the overall study. To obtain maximum sensitivity, the lowest full-scale sensitivity setting above the yarn strength under test was selected.

Breaking strength data are recorded in Appendix B, Table IX.

Elongation. Ultimate elongation was measured from the same charts obtained for the breaking strength tests. The chart is driven vertically downward at a known rate of speed as the load is being applied so that the vertical distance from the onset of loading to the breaking point is related to the amount of stretch undergone by the yarn during this period. In this study, the chart speed (10 in/min), was double that of the jaw speed (5 in/min), so elongation as indicated by the recorded curves was twice the actual elongation.

Most of the results reported are in terms of percentage elongation which was calculated by dividing the corrected elongation from the charts by the gage length and multiplying by 100. Elongation data are recorded in Appendix B, Table X.

Work-To-Break. The load-elongation curves obtained by the methods described under Breaking Strength were used again to calculate total energy capacity or work-to-break.

Initial tests were run with the Instron Integrator attachment included in the set-up to provide energy data. Possibly due to a faulty Integrator unit, these results were found to be inaccurate when checked by planimeter measurement. The planimeter method was, therefore, employed to measure the area bounded by all the curves, which were converted to energy units by the following relationship:

$$1 \text{ in}^2 = (.105 \times R)\ (1 \times \frac{JS}{CS}) \qquad (6)$$

where: R = Full-scale range
JS = Jaw Speed
CS = Chart Speed

Work-to-break data are recorded in Appendix B, Table XI.

(2) High Strain Rate. Test Apparatus. The test instrument used to make the high strain rate yarn tests is the FRITS Tester (Figure 1). This instrument has a maximum load capacity of 250 pounds and is capable of providing a maximum jaw speed of approximately 40 ft/sec. A continuous load-elongation trace of the specimen response is electronically transferred to an oscilloscope.

Power System. The rapid extension rates associated with the FRITS Tester are achieved by driving a piston in an enclosed cylinder with compressed nitrogen gas. The gas is introduced suddenly to the top of the cylinder, creating an excessive pressure above the piston and driving it downward. The downward motion is translated to the lower jaw of the tester through the piston rod to which it is connected.

The driving force exerted by the nitrogen gas on the piston is proportional to the pressure of the gas introduced:

$$F = PA \tag{7}$$

where: F = Force (lb)
P = Pressure (psi)
A = Effective gross sectional area of driving piston (in^2)

The force necessary to break a given sample may be obtained by adjusting the input pressure to the required level with a pressure regulator.

Variation of the input pressure also influences the velocity at which the lower jaw is driven. The effect of input pressure on velocity is usually of major interest, since sufficient force to rupture most samples is generated at relatively low pressures. The relationship between input pressure and piston velocity is shown in Figure 2.

Speeds above approximately 25 ft/sec are attainable (Figure 2), but are impractical due to the structural failures which would result from the shearing forces created by the abrupt bottoming of the piston at the end of its stroke.

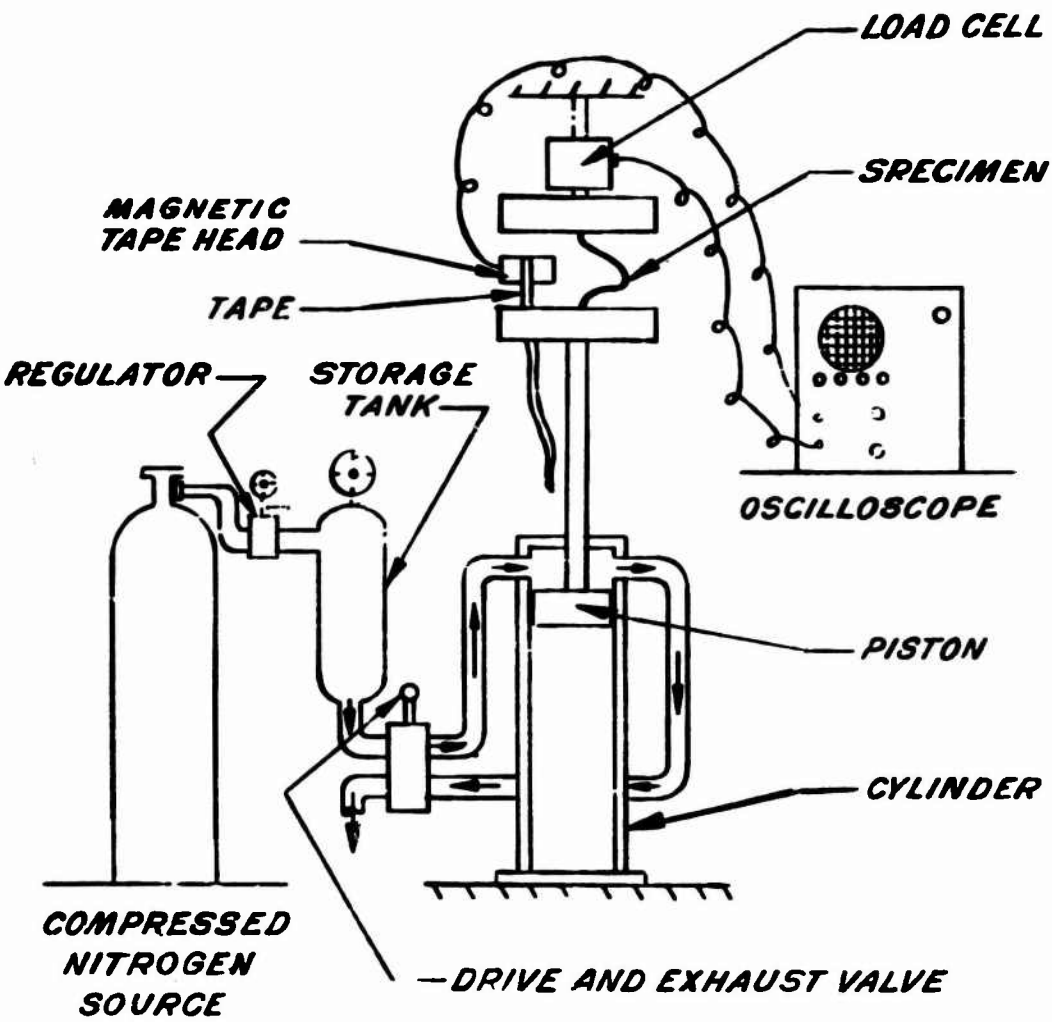

FIGURE 1 -SCHEMATIC SKETCH OF FRITS TENSILE TESTER

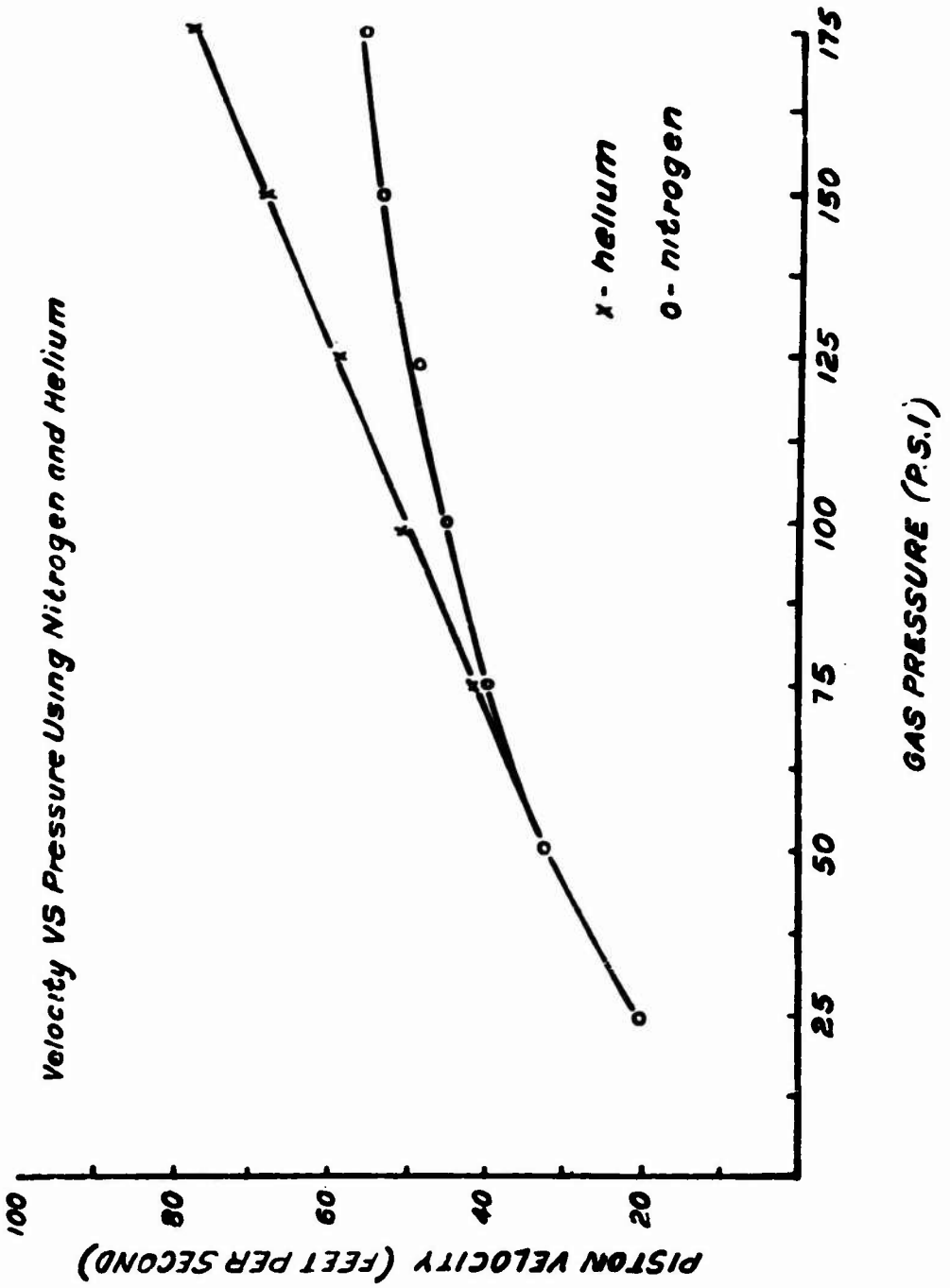

FIGURE 2-CALIBRATION CURVE FOR FRITS TESTER

The desired input pressure is easily obtained by adjusting the output pressure from a large cylinder of compressed nitrogen with a pressure regulator. Gas at this pressure is fed to a reservoir tank component of the instrument. When the test is to be made, a firing handle is pulled rapidly forward from its neutral position. This opens a valve which allows the gas at the set pressure to rush from the reservoir to the cylinder and drive the piston. The handle is pushed backward from its neutral position after the test, opening a valve which exhausts the gas from the cylinder. The jaw can then be raised manually, with the handle in the exhaust position, for the next test. Driving pressure in the reservoir remains constant so that consistency in jaw velocity is obtained from test to test.

Determination of the actual velocity of the jaw during loading of the specimen is not merely a matter of reading from a chart such as Figure 2, which shows the velocity associated with a given pressure. It must be recognized that this drive system moves a mass from a zero initial velocity through an uncontrolled acceleration and deceleration during the complete piston stroke. It is, therefore, necessary to measure the velocity over a particular short distance of its stroke during which the specimen is under load. The instrumentation employed in this set-up allows such a measurement.

Instrumentation. At the test speeds associated with the FRITS instrument, the complete loading to rupture of a specimen is accomplished extremely rapidly (in the order of milliseconds). It is, therefore, necessary to record specimen response with more sensitive devices than those normally used at conventional speeds. The instrument system used consisted of an electronic load cell for measuring force and a magnetic tape recorder head for measuring jaw displacement.

The load cell was a Shaevitz-Bytrex type JP-200. This was attached to the upper jaw by a short threaded rod running to the bottom of the cell, and to the tester frame by a threaded rod from the top of the cell. The load cell is designed internally as an "L"-shaped structure with four wire strain gages bonded to its members, providing a Wheatstone bridge circuit. During loading of the specimen, the force is imparted to the horizontal member of the "L" causing a mechanical deflection of the structure and an unbalancing of the Wheatstone Bridge circuit. This results in a voltage output from the cell. The load cell has a maximum capacity of 200 pounds; forces exceeding 200 pounds will cause permanent deformation of the "L" structure with subsequent non-elastic cell behavior and permanent bridge circuit unbalance under no-load conditions.

The voltage output from the load cell during normal loading is fed to one channel of a dual-beam oscilloscope (Tektronix, Model 502). With additional load the rising voltage continually increases the vertical displacement of a base signal on the oscilloscope screen. Since the base signal is sweeping horizontally across the screen, the increasing displacement is traced across the screen as a typical stress strain curve (Figure 3). A permanent record of the event, such as is shown in Figure 3, is obtained by photographing the oscilloscope screen with a Polaroid camera at a lens opening time sufficient to record the entire loading from no-load to rupture. The flat no-load portion at the beginning (left) of the sweep is used as a reference for measuring the total vertical displacement distance at the rupture point or at any point along the curve. This base reference is essential for evaluation of results.

The second channel of the dual-beam oscilloscope provides a trace which sweeps across the screen at the same rate as the load trace. A signal fed to this channel provides information from which elongation and jaw velocity can be calculated. The signal comes from a tape recorder head attached to the tester and wired to the oscilloscope input. A tape which has been pre-recorded with a pip signal of known frequency is passed over the tape head and attached to the lower moving jaw of the tester. The tape moves with the jaw and passes the tape head, which picks up the pre-recorded pips and sends them to the oscilloscope. Since the pre-recorded tape signal was of a known frequency, the distance between pips represents a known consistent spacing along the tape, which now corresponds to the distance travelled by the jaw.

Total elongation can then be computed by measuring the distance from the onset of loading to the rupture point on the upper load curve in comparison to the corresponding number of peaks of the lower motion curve: the peak-to-peak displacement (Figure 3) represents 0.1-inch of jaw travel. One centimeter of vertical displacement on the loading curve represents 7.15 pounds. This value and the ultimate load display may vary with changes in oscilloscope sensitivity, which is adjustable as desired; load cell excitation voltage, also adjustable through a d.c. power supply unit; and characteristic load cell sensitivity, which may vary slightly with temperature and excitation voltage. Load output under any conditions may be calculated by the following relationship:

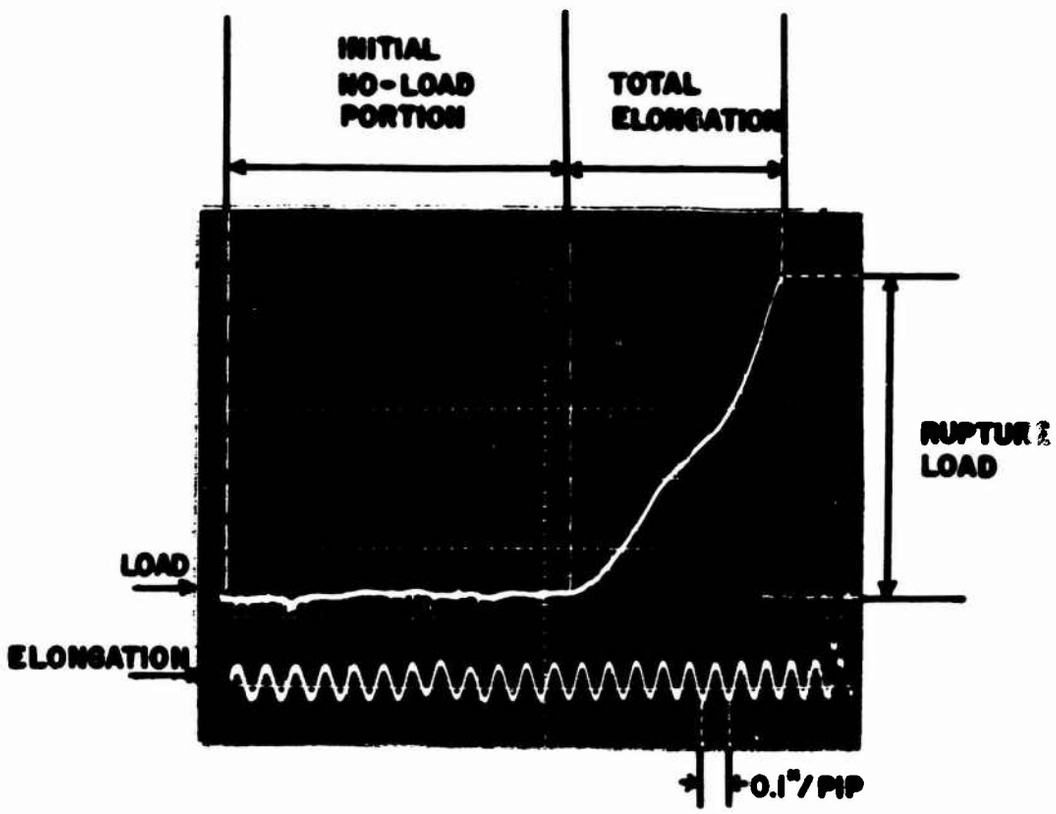

FIGURE 3 - TYPICAL PHOTOGRAPHIC RECORD OF HIGH STRAIN RATE TEST

$$\text{Load (lb)} = \frac{l(\text{cm}) \times \text{O.S.} \left(\frac{\text{mv}}{\text{cm}}\right) \times \text{L.C.C.} (\text{lb})}{\text{E. V.} \quad (\text{V}) \times \text{L.C.S.} \left(\frac{\text{mv}}{\text{v}}\right)} \qquad (8)$$

where: O.S. = oscilloscope sensitivity setting ($\frac{\text{millivolts}}{\text{centimeter}}$)
L.C.C. = load cell capacity (200 lbs. for this study)
E.V. = load cell excitation voltage (5 volts for this study)
L.C.S. = load cell sensitivity (normally 28 $\frac{\text{millivolts}}{\text{volt excitation}}$)

Breaking Strength. As mentioned previously, the downward motion of the lower jaw of the FRITS Tester varies in speed during the 12 inches of piston stroke. For this reason, breaking strength specimens cannot be clamped into the jaws in a taut condition since the loading would take place during the initial acceleration portion of the stroke when jaw velocity is continually increasing. A method was devised which would allow loading after approximately three inches of piston stroke when the jaw velocity was more constant.

This was done by placing the fully twisted yarn samples on a table directly over gage marks which were five inches apart. A pretension weight of 11.1 grams was hung on the end of the yarn extended over the table edge, and tape was placed across the yarn at the five-inch gage marks. The yarn could then be removed from the table with the tapes still attached at the gage points. The two gage points were then clamped at the edges of the upper and lower jaws.

The distance between jaws was only two inches, however, so three inches of slack yarn remained between the jaws. In this way no loading took place while the slack in the specimen was being taken up, and the jaw was allowed to accelerate to a fairly constant velocity during the initial three inches of stroke. Through this method, excellent consistency was maintained in loading velocity from test to test.

In order to assure successful photographic records of the specimen behavior, the loading must be synchronized with one sweep of the oscilloscope signal across the screen (10-20 milliseconds). This signal was triggered externally just prior to complete sample slack takeup. Thus a no-load base reference signal at the left of the photograph was followed by the typical stress-strain curve traced from left to right.

Five specimens were tested for each yarn structure. Breaking strength or load at any point along the curve could be obtained from the permanent photographic record by the use of equation (8).

Raw data are recorded in Appendix B, Table IX.

Elongation. By the methods employed in the previous section, consistent jaw velocities of 20 ft/sec were maintained during the loading portion of the stroke for all specimens. This resulted in an extension rate on the sample of 288,000%/min by the following relationship:

$$E.R. = \frac{J.V.}{G.L.} \times 72{,}000 \qquad (9)$$

where: E.R. = extension rate (%/min)
J.V. = jaw velocity (ft/sec)
G.L. = gage length (inches)

From the Polaroid print records obtained, elongation could be measured by transferring the horizontal distance from the onset of loading to the rupture point to the lower trace of displacement pips with a pair of dividers. The number of pips included in the distance were counted to the nearest 0.1 pip. The distance could then be easily converted to elongation by:

$$\text{Elongation } (\%) = \frac{P}{GL} \times 10 \qquad (10)$$

where: P = number of pips
G.L. = gage length (in.)

The constant multiplier, 10, in the above expression is obtained by multiplying the distance represented by one pip (0.1-inch) by 100%.

Equation (10) may also be used to determine the number of pips required to attain a particular elongation level when calculating stress-strain data for re-plot.

Elongation data are recorded in Appendix B, Table X.

Work-to-Break. Determination of the energy-absorbing capacity of the yarns at high strain rate required a planimeter to measure the surface area under each load-elongation curve and proper conversion of these measurements into energy units.

Conversion from plane area to inch-pounds may be best understood by treating a square inch of surface first as a one-inch horizontal displacement, (yielding inches), and then as a one-inch vertical displacement, (yielding pounds).

$$1\ \text{inch}_{(\text{horiz.})} = 2.54\ \text{cm} \times \text{S.R.} \times \text{J.V.} \times .012 = \text{inches} \quad (11)$$

where: S.R. = signal sweep speed (milliseconds/cm)
J.V. = jaw velocity (ft/sec)

$$1\ \text{inch}_{(\text{vert.})} = \frac{2.54\ \text{cm} \times \text{O.S.} \times \text{L.C.C.}}{\text{E.V.} \times \text{L.C.S.}} \quad (12)$$

The product of equations (11) and (12) gives the equivalent of one square inch in terms of energy (in-lb)units. The combined expression for work-to-break then becomes:

$$\text{Energy (in-lb)} = A \times \frac{\text{S.R.} \times \text{J.V.} \times \text{O.S.} \times \text{L.C.C.}}{\text{E.V.} \times \text{L.C.S.}} \times .077 \quad (13)$$

where: A = Area under curve (in^2)

Measurements were made of every specimen tested. Data obtained are recorded in Appendix B, Table XI.

c. Yarn Denier

To plot stress-strain curves for analysis of curve shape differences, it was necessary to obtain the denier of each yarn in its particular final configuration. This was done by weighing specimens on a Mettler balance. Three separate 20-inch lengths of each yarn were prepared and weighed together. Readings were taken to the nearest 0.1 milligram. Conversion from grams per 5 feet to denier were made by multiplying by a factor of 5905.8.

Results are recorded in Appendix B, page 67.

d. Stress-Strain Curves

Data necessary for plotting of stress-strain curves were obtained from the original chart records of Instron tests and Polaroid prints from the FRITS Tester. Strength readings were taken from the original curves at intervals of 2% strain. These were then converted from pounds to specific stress (gpd) by appropriate calculation using the denier measurements made previously. Initial inflection points were also identified as accurately as possible.

One curve of the five available for each yarn was selected as most typical of the average behavior, and used for stress-strain computation. The results obtained for all yarns were plotted on one page so that changes in shape due to ply and twist could be easily followed.

4. Results and Discussion

a. Single Yarn Retraction (l_s)

The yarns investigated in this study were made up of two, three, five or seven single strands combined into a plied structure. In plying, the individual strands retract in proportion to the amount of ply twist added.

Computation of this retraction was accomplished through the use of Figure 4, which was prepared from the data obtained by twisting a single strand from zero through approximately 11 tpi and measuring retraction at various levels of twist.

The resultant yarn retractions were as follows:

2 tpi yarns	$l_s = .9994$
5 tpi yarns	$l_s = .9965$
9 tpi yarns	$l_s = .9888$

b. Ply Yarn Retraction (l_o)

Results for the retraction of the total ply with increasing twist are shown in Figure 5. Each point represents the average of three runs accomplished by downtwisting the yarns from their final twisted form to zero and measuring the increase in length. Uniform trends are noted, with retraction increasing as ply increases due to the increasing outer circumference.

c. Ply Helix Angle (α)

The ply helix angles measured microscopically are plotted against ply twist in Figure 6. The results are fairly uniform but a moderate to high degree of variation within some groups was noted (Appendix B, Table VI). The variability is believed to be largely inherent in the yarns, though a certain percentage is probably experimental error.

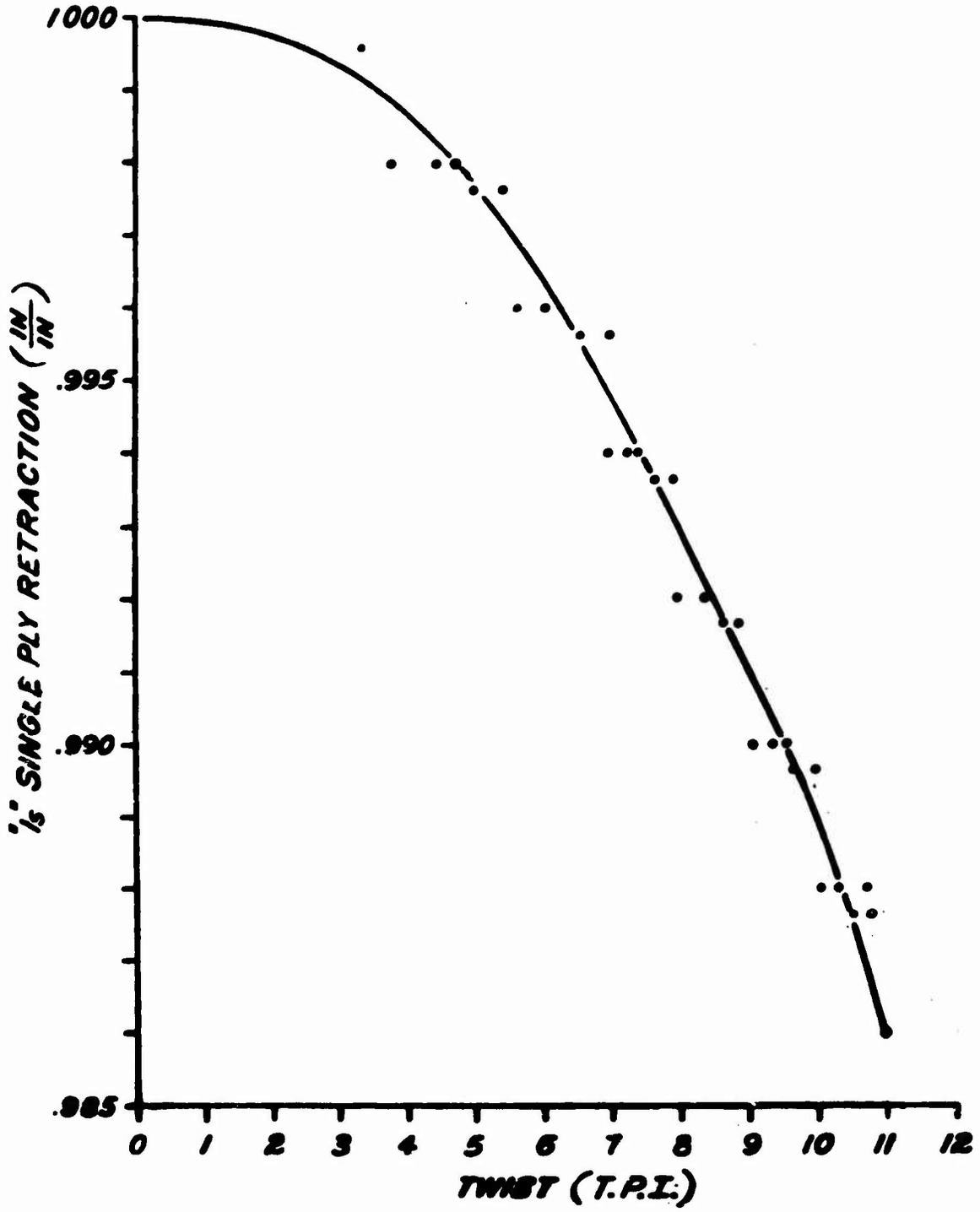

FIGURE 4-RETRACTION VS TWIST FOR SINGLE PLY, 210 DENIER, NYLON 66 YARN

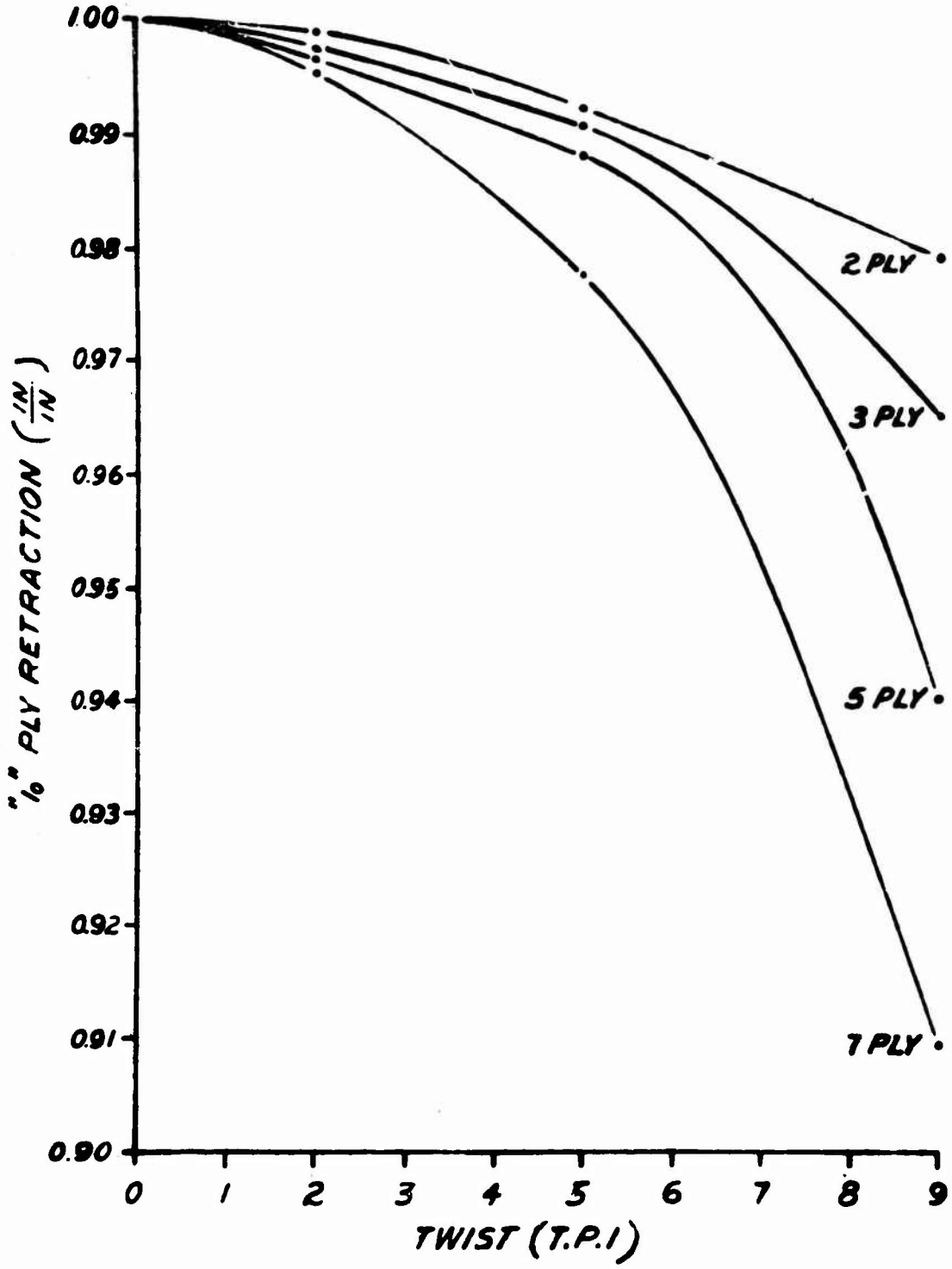

FIGURE 5-RETRACTION VS. TWIST FOR 210 DENIER, NYLON 66 YARN, PLIED TO VARIOUS LEVELS

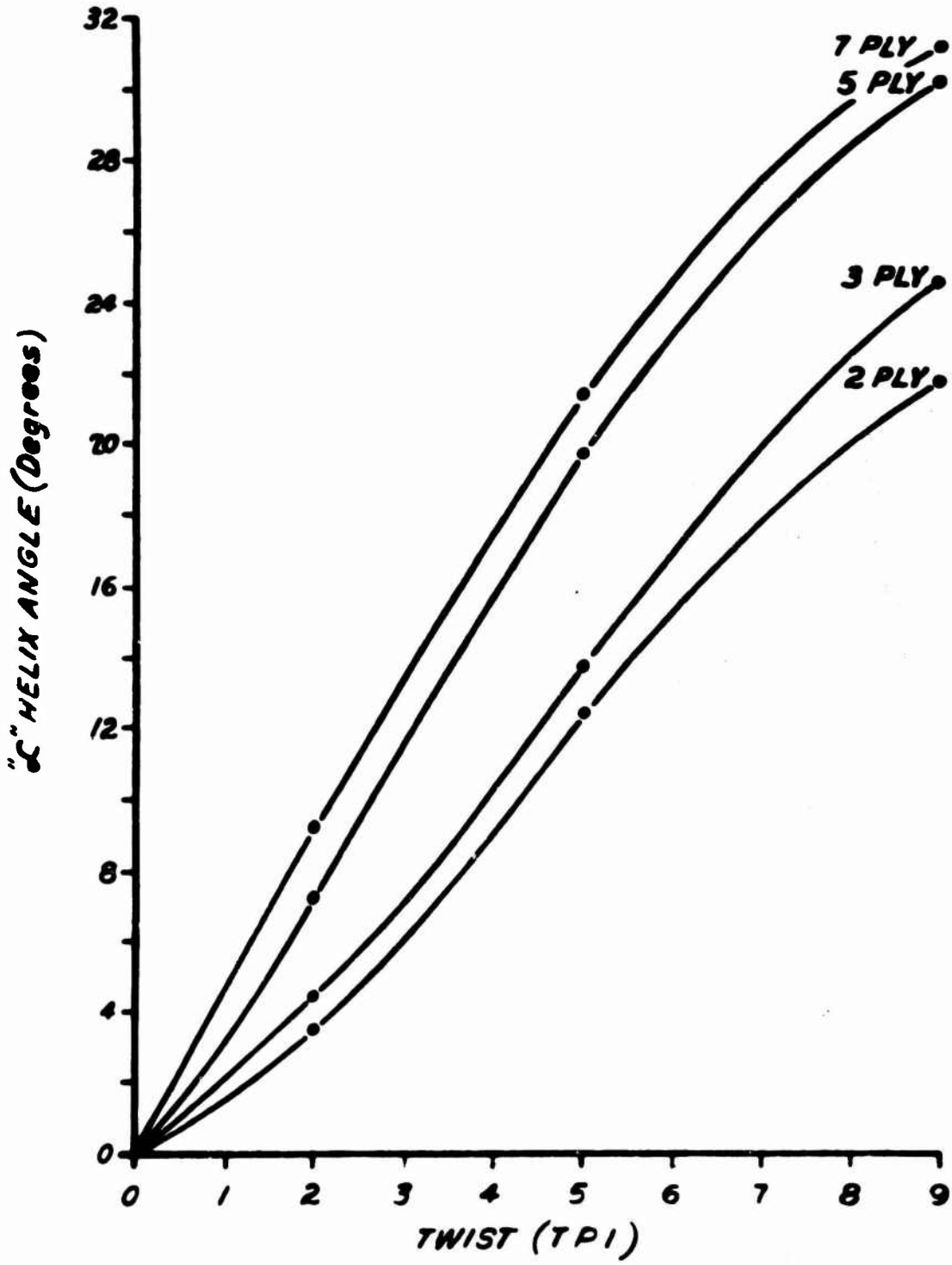

FIGURE 6 - HELIX ANGLE VS TWIST FOR 210 DENIER NYLON 66 YARN, PLIED TO VARIOUS LEVELS

d. Ply Radius (a_o)

Ply radius was calculated from equations (4) and (5), employing the theoretical correction factors presented by Schwarz.

Ply diameter and radius are dependent upon two opposing effects which take place during the plying operation. One is the tightening effect of increasing twist which tends to decrease the diameter. The other is the yarn retraction with twist which tends to increase the diameter. The extent to which one of these effects may predominate is dependent upon other factors such as bulk density, packing coefficient, and buckling of the yarns.

Figure 7 shows that radius increases with twist for two and three-ply yarns, indicating that yarn retraction exerts the major influence at the lower ply levels. The radius of the seven-ply yarn decreases with twist despite the fact that it showed the greatest ply yarn retraction (Figure 6). This suggests that its packing coefficient was less, allowing the yarn to be more easily compressed. The five-ply seems to be at a transition level which behaves as the lower plies up to five tpi and then is more like the seven-ply as the twist is further increased.

e. Ply Torsion (ψ_o)

Equation (1) for total torsion of the plied yarn is repeated here for clarity.

$$\psi_o = \psi_s \frac{l_s}{l_o} + \frac{1}{a_o} \sin\alpha \cos\alpha \qquad (1)$$

where: ψ_o = total ply torsion
ψ_s = single yarn torsion
l_s = single yarn retraction
l_o = ply yarn retraction
a_o = ply radius
α = ply helix angle

The total torsion of the plied yarn is the sum of the torsion of the single yarn about its own axis (represented by the $\psi_s \times l_s/l_o$ term in equation (1)), and the remainder of the expression ($\sin\alpha \cos\alpha / a_o$) which represents the tortuosity of the helix axes formed by the individual plies about the principal axis of the yarn. (The physical interpretations of torsion and tortuosity are explained in

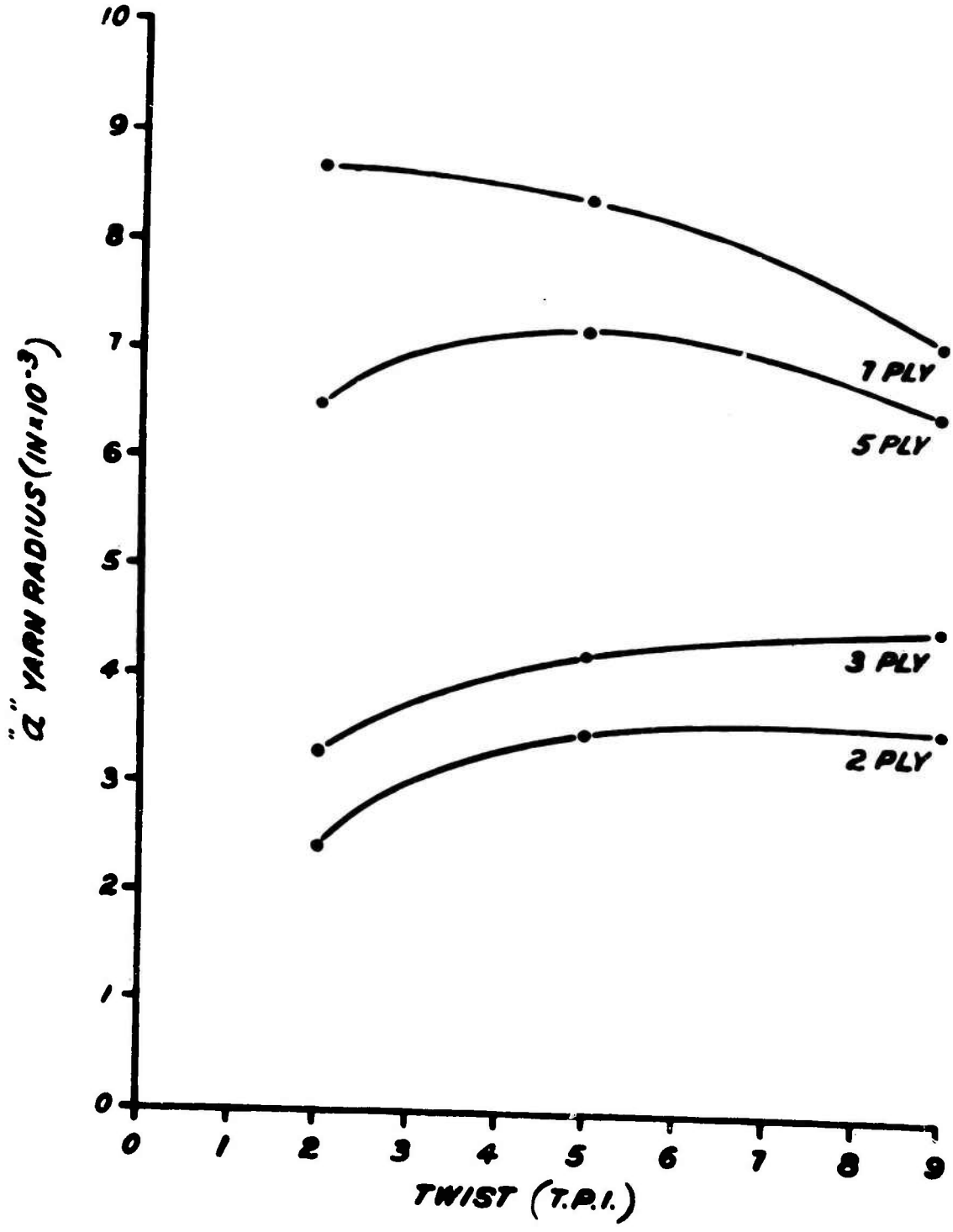

FIGURE 7 - PLY AXIS RADIUS VS. TWIST FOR 210 DENIER, NYLON 66 YARN, PLIED TO VARIOUS LEVELS

Appendix A). The single yarn torsion Ψ_s contributes less than half of the total yarn torsion. Its value increases from approximately 17 to 61 as twist is increased from 2 to 9 tpi (see Appendix B, Table VIII). Adjustment of the Ψ_s value by the l_s/l_o ratio is very small. The effects of this correction is to increase Ψ_s as ply and twist increase.

The tortuosity portion of the relationship ($\sin\alpha \cos\alpha / a_o$) brings into play the interaction of ply helix and radius. It contributes the larger portion of the total yarn torsion.

The results obtained for total ply torsion, Ψo,, are plotted against twist in Figure 8. These show that at each ply level the torsion increases as twist is increased, which reflects increases in single yarn torsion with twist, and a predominance of increasing helix over relatively stable yarn radius.

Reduction in total torsion due to additional plying is also noted in Figure 8. This is attributed to the effect of increasing yarn radius with increased ply.

f. Breaking Strength.

Figure 9 shows breaking strength at both high and low strain rate for all ply yarns studied. It is seen that breaking strength at low strain rate becomes greater as ply level is increased, as would be expected. However, the increases are not in proportion to the increases in ply number. The low-speed breaking strength for each ply at its lowest torsion increases from 6.7 pounds at 2-ply to 10.2 pounds, 16.9 pounds, and 24.1 pounds at 3, 5, and 7-plies, respectively. Moreover, compared with a single strand strength of 3.5 pounds at low strain rate, the strength efficiency is less than 100% at all ply levels, i.e., two-ply yarn would be expected to break at 7.0 pounds (2 ply x 3.5 lbs/strand). This indicates that some translational effect has taken place due to plying.

Similarly, the breaking strengths at high strain rate, although greater than those at low speed, also have efficiencies below 100% as compared with their single strand strength of 4.5 pounds at high strain rate.

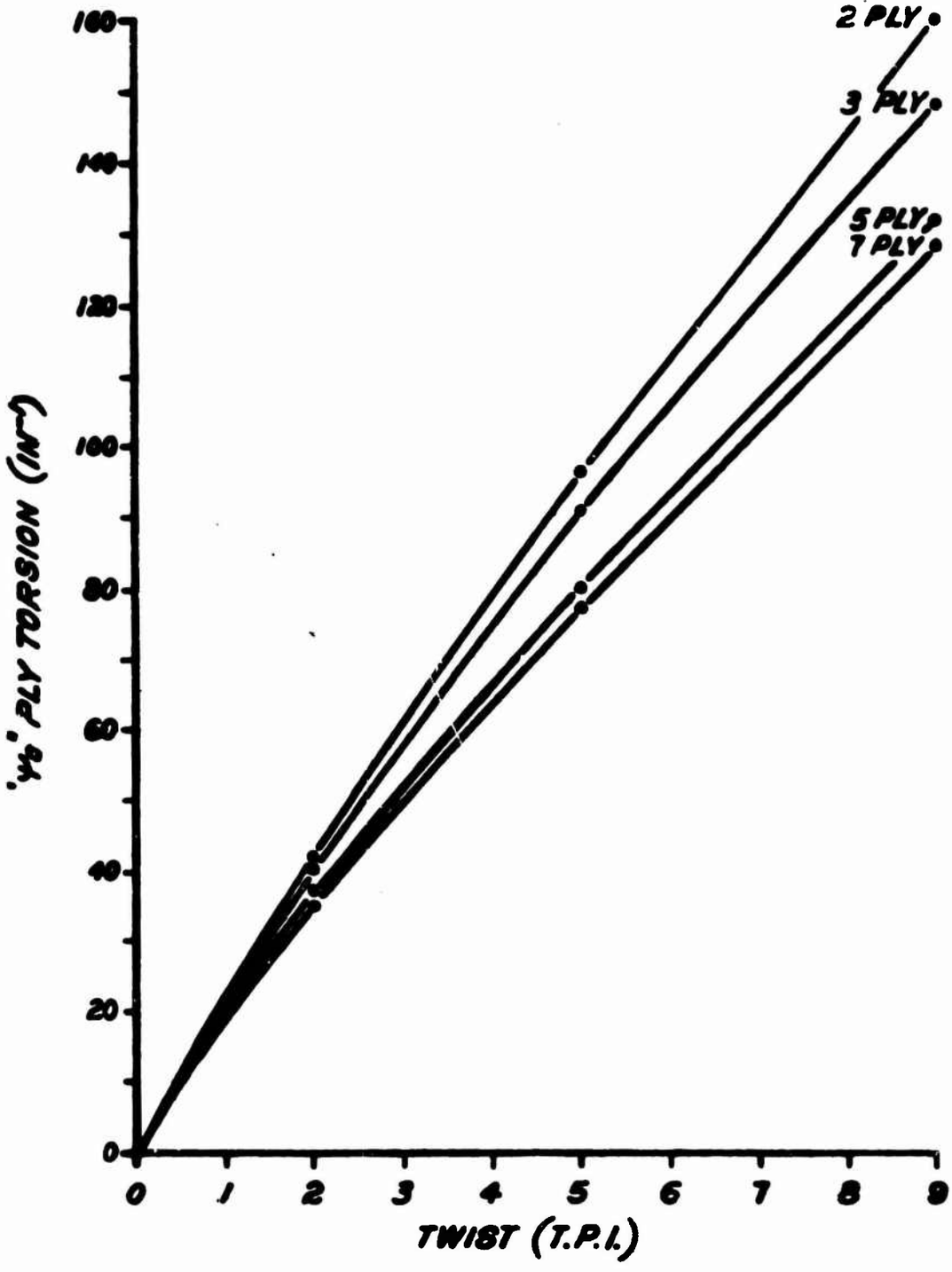

FIGURE 8 -PLY TORSION VS. TWIST FOR 210 DENIER, NYLON 66 YARN, PLIED TO VARIOUS LEVELS

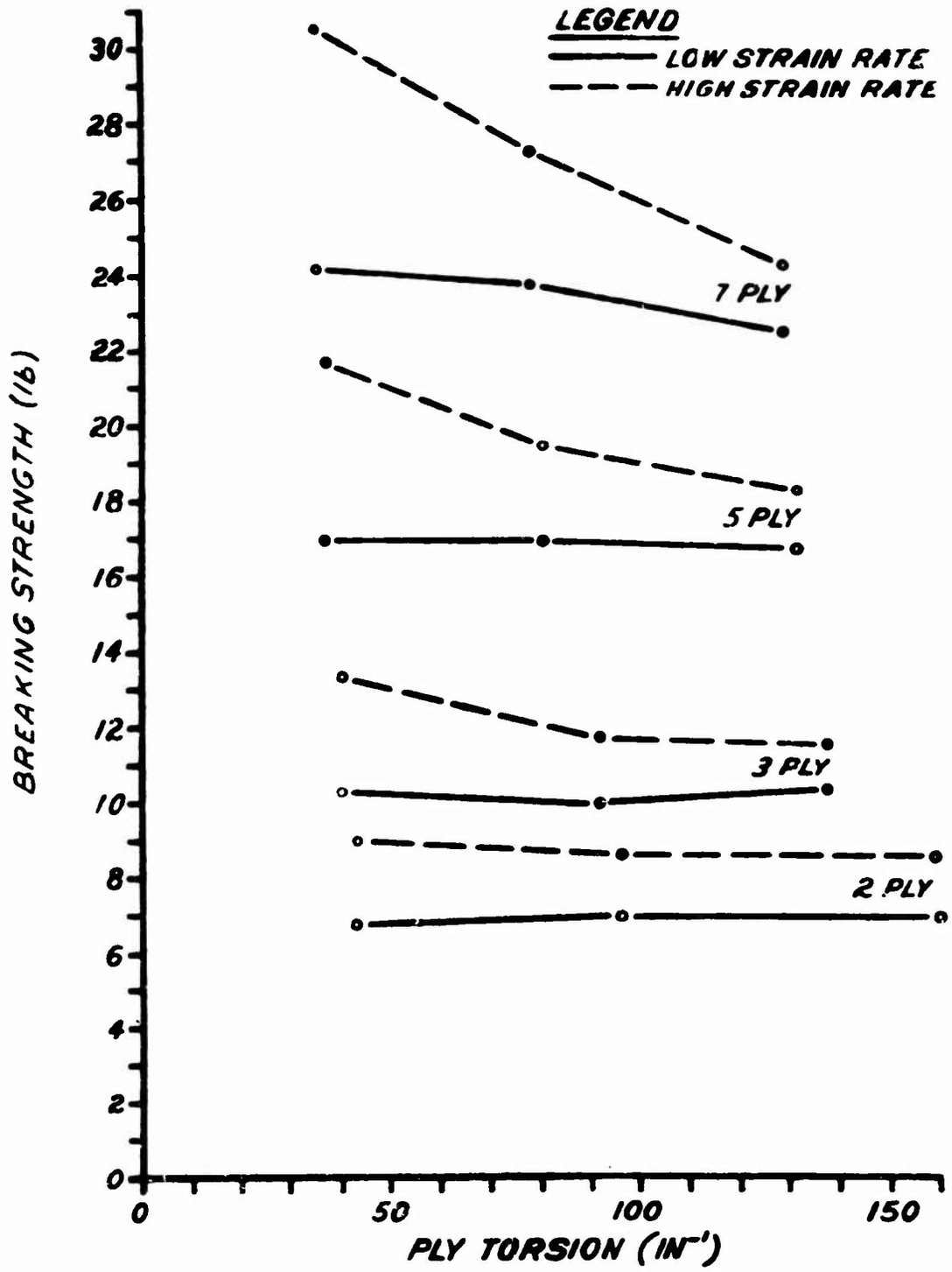

FIGURE 9-BREAKING STRENGTH AT HIGH AND LOW STRAIN RATES VS. PLY TORSION FOR NYLON 66 PLIED YARNS

Table I lists strength efficiencies for all structures at both strain rates. From this, the effects of ply, twist and strain rate can be more easily followed.

It is seen that at the low speed, 100% efficiency is not attained at any level of complexity. The results are quite uniform with little effect of plying or twisting noted throughout the yarn series. The most complex structure (7 ply-9 tpi) had the lowest efficiency (92%), but this is not a serious loss.

High strain rate results, on the other hand, were more sensitive to structural changes. Progressive losses occurred due to increases in ply and also to increases in twist within ply groups. The translational inefficiencies set up in the various yarn forms are also more serious at this strain rate, as is indicated by the generally lower efficiency values throughout.

It is this accentuation of the translational effect under conditions of rapid loading which is considered most significant and which must be more clearly defined through the study of geometric interactions under these conditions.

A further analysis of the relative behavior at the two strain rates is shown in Figure 10. Here the ratio of high-speed to low-speed breaking strength was computed for each structure and plotted against the corresponding ply torsion. If the level of translation efficiency attained in a tensile test were considered in terms of internal time-dependent readjustments within the mechanical structure, and then the ratio used here would compare the ability of the structure to readjust under rapid loading conditions with its ability to adjust under slow rates. Therefore, decreasing trends in Figure 10 would indicate that as torsions increase, adjustment comparable to that under slow loading becomes more and more difficult. Such tendencies are noted and are seen to fall into a fairly uniform pattern. The generalized behavior may be described mathematically by a relationship of the form:

$$y = ae^{-bx} + c \qquad (14)$$

or, in terms of this study:

$$\frac{BS_{HS}}{BS_{LS}} = ae^{-b\Psi_o} + c \qquad (15)$$

TABLE I

STRENGTH EFFICIENCY OF NYLON PLIED YARNS

AT HIGH AND LOW STRAIN RATES

	Low Strain Rate (100%/min)			High Strain Rate (288,000 %/min)		
	Actual BS(lb)	Theoretical BS(lb)	Efficiency %	Actual BS(lb)	Theoretical BS(lb)	Efficiency %
Single Ply	3.5	-	-	4.5	-	-
2 ply 2 tpi	6.7	7.0	95.5	9.1	9.0	100.0
2 " 5 "	6.8	"	97.0	8.5	"	94.5
2 " 9 "	6.9	"	98.5	8.5	"	94.5
3 " 2 "	10.2	10.5	97.5	13.3	13.5	98.5
3 " 5 "	9.9	"	94.5	11.6	"	86.0
3 " 9 "	10.3	"	98.5	11.6	"	86.0
5 " 2 "	16.9	17.5	96.5	21.6	22.5	96.0
5 " 5 "	16.9	"	95.5	19.5	"	86.5
5 " 9 "	16.7	"	95.5	18.3	"	81.5
7 " 2 "	24.1	24.5	98.5	30.6	31.5	97.0
7 " 5 "	23.8	"	97.5	27.3	"	84.5
7 " 9 "	22.5	"	92.0	24.2	"	77.0

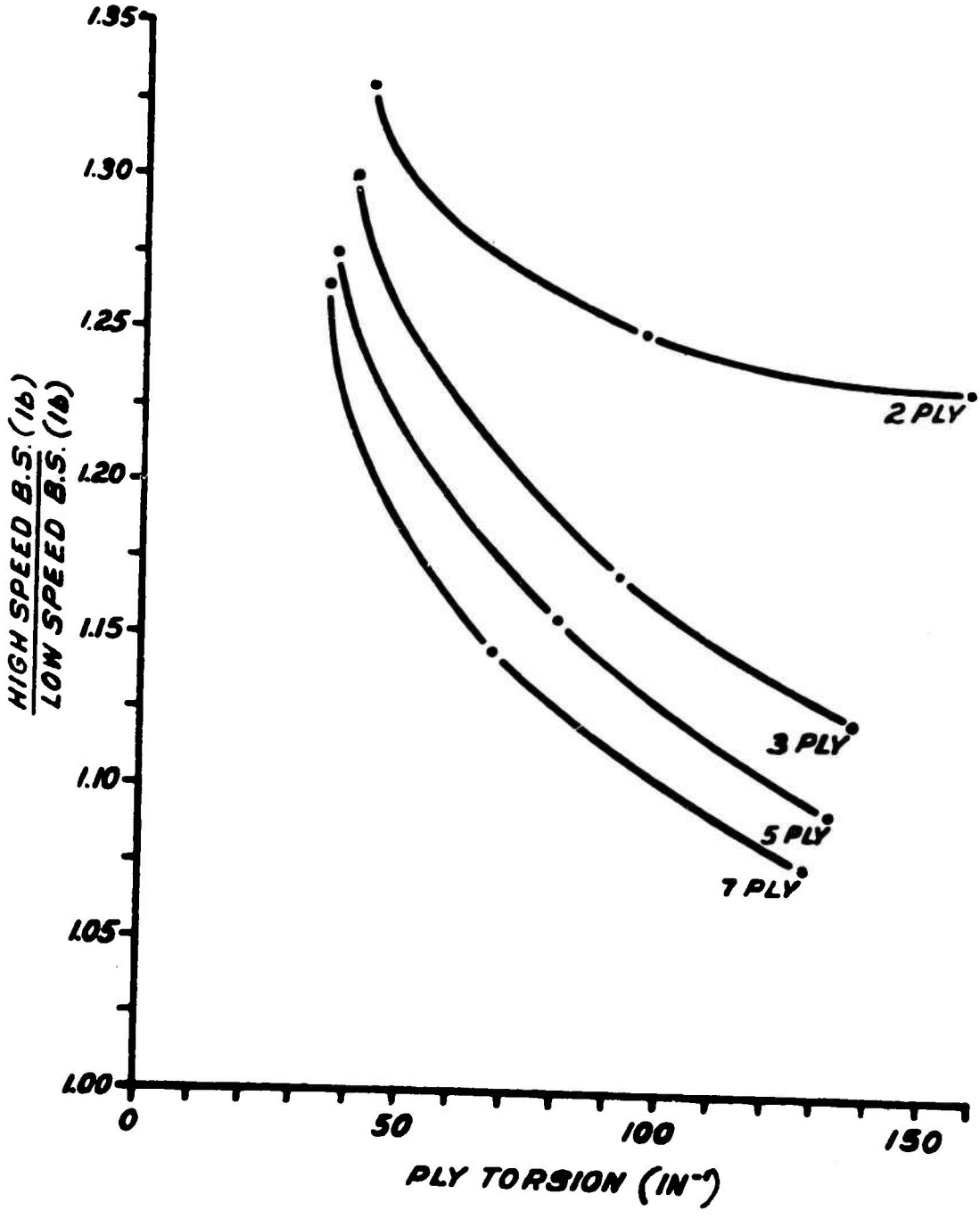

FIGURE 10 - BREAKING STRENGTH RATIO VS. PLY TORSION FOR NYLON 66 PLIED YARNS

where: BS_{HS} = High strain rate breaking strength
BS_{LS} = Low strain rate breaking strength
Ψ_o = Ply Torsion
a,b,c = Constants

By appropriate analysis (see Appendix B, page 68) the following relationships were derived:

2 ply yarn: $BS_{HS} = BS_{LS} (0.460\ e^{-.00264\Psi_o} + .91)$ (16)
3 ply yarn: $BS_{HS} = BS_{LS} (0.425\ e^{-.01483\Psi_o} + 1.071)$ (17)
5 ply yarn: $BS_{HS} = BS_{LS} (0.443\ e^{-.01913\Psi_o} + 1.058)$ (18)
7 ply yarn: $BS_{HS} = BS_{LS} (0.427\ e^{-.01400\Psi_o} + 1.000)$ (19)

g. Elongation.

Figures 11 and 12 show the elongations at rupture for the yarns at low and high strain rates, respectively.

The trends at both strain rates are generally similar, with elongations increasing as ply and torsion increase. However, a notable exception to this trend occurs at high strain rate where the two and three-ply curves are out of sequence. One factor which may have contributed to this reversal is error in interpretation of the Polaroid print records for these tests. Since the strength levels associated with these two and three-ply yarns are relatively low, extreme sensitivity was required in the instrumentation to obtain reasonable output in the load curves. This sensitivity was such that vibrations within the test instrument were also picked up and recorded, producing a great deal of noise along with the initial no-load position at the left of the trace (Figure 3) which is normally a steady horizontal signal. This garbled reference signal made it difficult in many cases to ascertain the exact point at which the onset of loading took place and, therefore, the point from which elongation was to be measured.

Assuming that interpretations of the data curves were correct and that this reversal is valid, a possible physical explanation may then be offered. A possibility would be that a corkscrew of two plies about the third took place. Elongation at low strain rate would probably still be normal, or in sequence, because sufficient time for reorientation was allowed. However, at rapid loading insufficient adjustment time would make the elongation effectively that of a single strand. A double corkscrew is unlikely, however, and it is more unlikely that a double corkscrew would have occurred in all three-ply yarns tested.

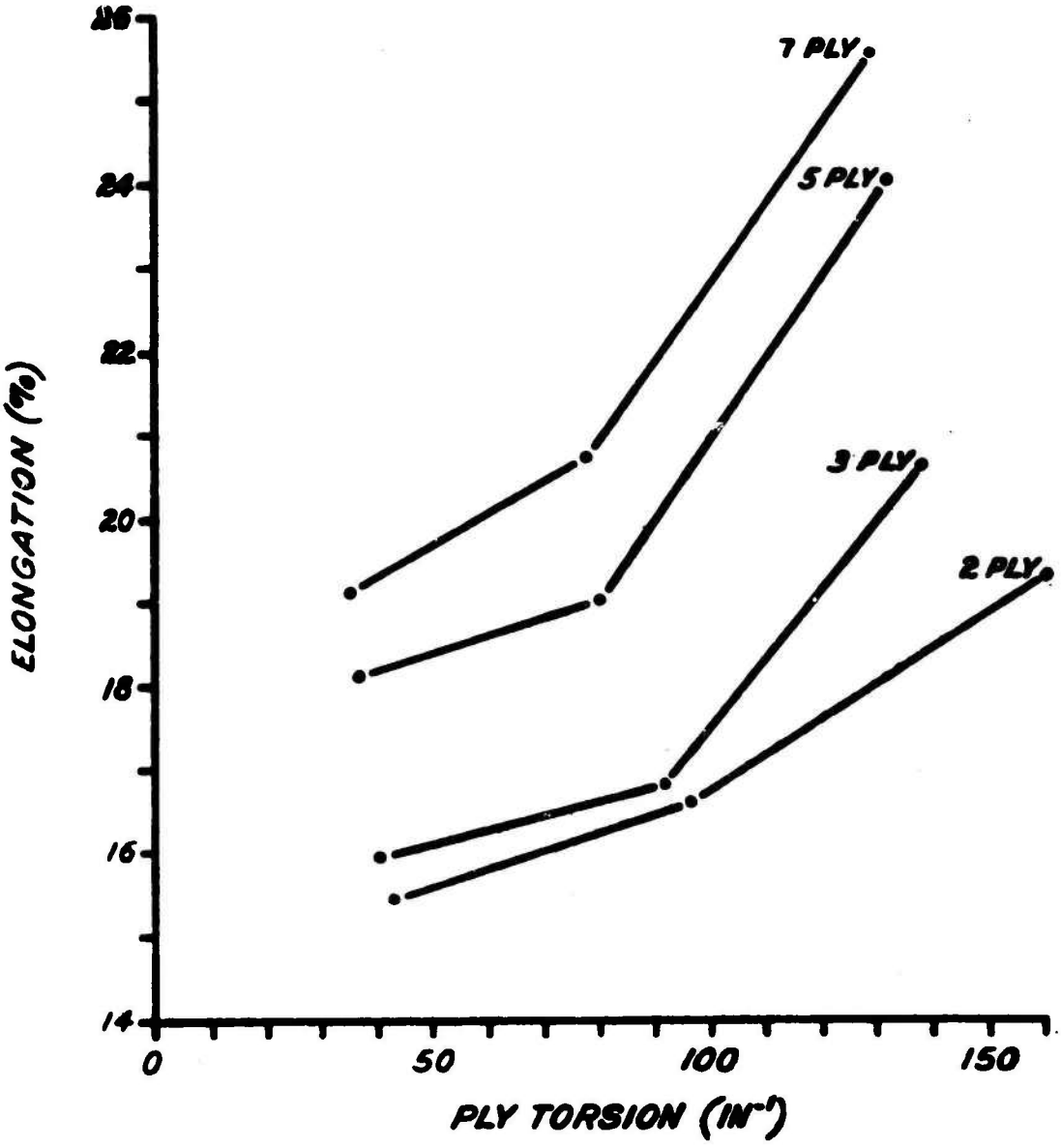

FIGURE 11 -ULTIMATE ELONGATION AT LOW STRAIN RATE VS PLY TORSION FOR NYLON 66 PLIED YARNS

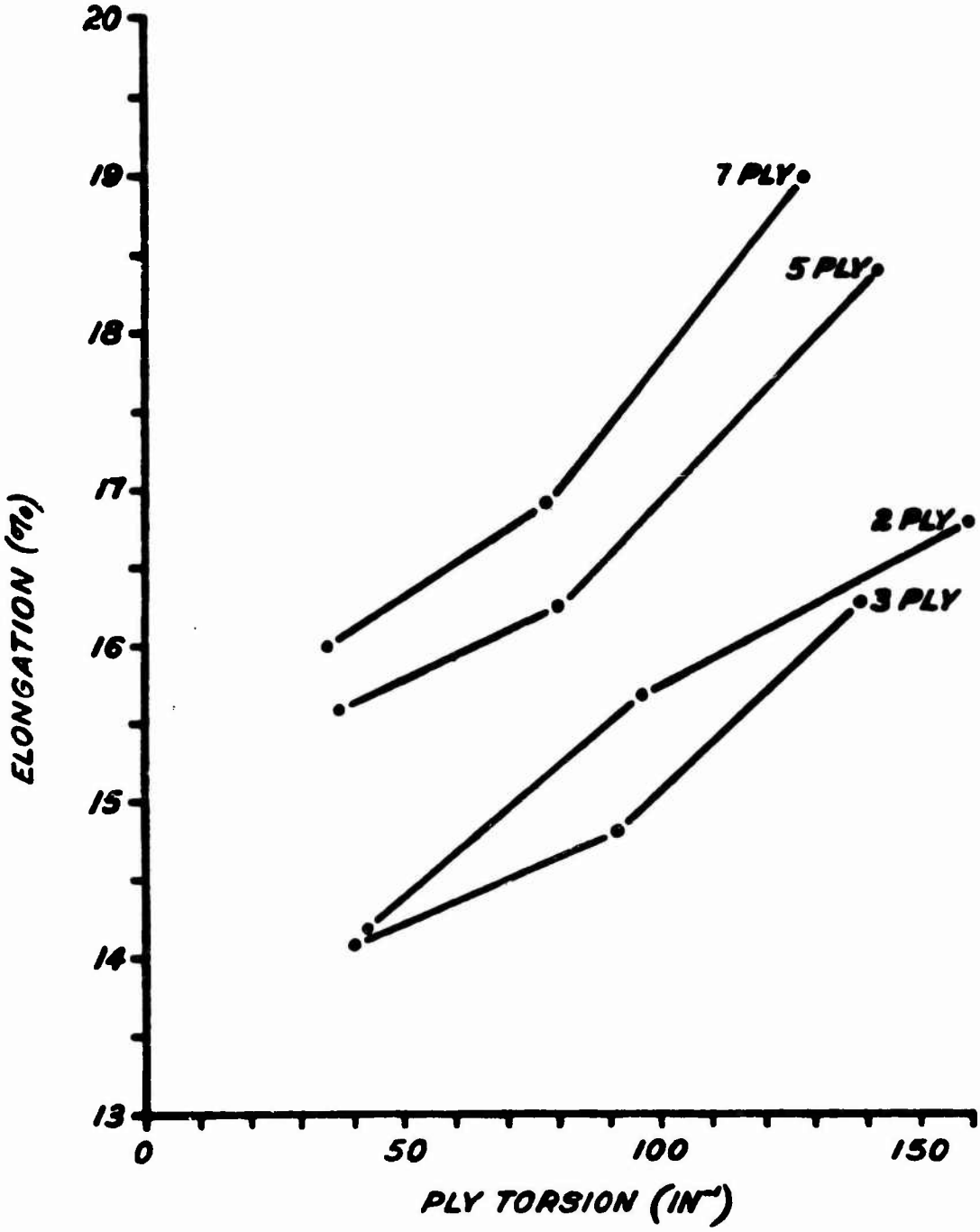

FIGURE 12 - ULTIMATE ELONGATION AT HIGH STRAIN RATE VS PLY TORSION FOR NYLON 66 PLIED YARNS

The most significant observation made when comparing elongations at the two strain rates is that at all levels of torsion, the elongations at impact are less than those at slow speed; as ply and torsion are increased, the elongations at impact become increasingly less than those at slow speed. Table II illustrates this trend. These results show that the elongation potential inherent in the twisted ply structure is not utilized at high speed to the extent that it is at low speed, and that this unused capability is progressive with increased ply and torsion. This behavior resembles that observed in the analysis of strength results.

As was done in the strength analysis, a ratio of high to low strain rate elongation was computed for all yarns and plotted against the corresponding yarn torsions (Figure 13). These curves also fall into a fairly uniform pattern with the exception of the two-ply curve which will not be included in the following mathematical treatment.

(1) Work-To-Break. The total performance capability of a yarn is best described by its work-to-break, or its ability to absorb energy. The interaction of stress and strain described through this parameter is particularly meaningful where they are changing in various directions as strain rate and geometry vary.

It was noted previously that yarn strength is greater at high speed than at low speed, but it becomes decreasingly so as structure becomes more complex.

It was also noted that yarn elongation is lower at high speed than at low speed and becomes increasingly so as structure becomes more complex.

Figure 14 shows that for two-ply yarns the work-to-break at high strain rate is slightly greater at the lowest torsional level and slightly lower at the highest level. The small difference in values at the two strain rates is in keeping with the relatively simple structural form and is analogous to results for single-ply yarns (Table III), in which work-to-break is also essentially the same at both strain rates. A pattern begins to form at the two-ply level, however, with the high speed values dropping below the low speed values as torsion increases.

TABLE II

ELONGATION OF NYLON PLIED YARNS: DIFFERENCES BETWEEN HIGH AND LOW STRAIN RATE (PERCENT)

	Low Strain Rate (100%/min)	High Strain Rate (288,000%/min)	Difference (Low-High)
2 ply 2 tpi	15.5	14.2	1.3
2 " 5 "	16.6	15.7	0.9
2 " 9 "	19.3	16.8	2.5
3 " 2 "	16.0	14.1	1.9
3 " 5 "	16.8	14.8	2.0
3 " 9 "	20.6	16.3	4.3
5 " 2 "	18.1	15.6	2.5
5 " 5 "	19.0	16.3	2.7
5 " 9 "	24.0	18.4	5.6
7 " 2 "	19.0	16.0	3.1
7 " 5 "	20.7	16.9	3.8
7 " 9 "	25.5	19.0	6.5

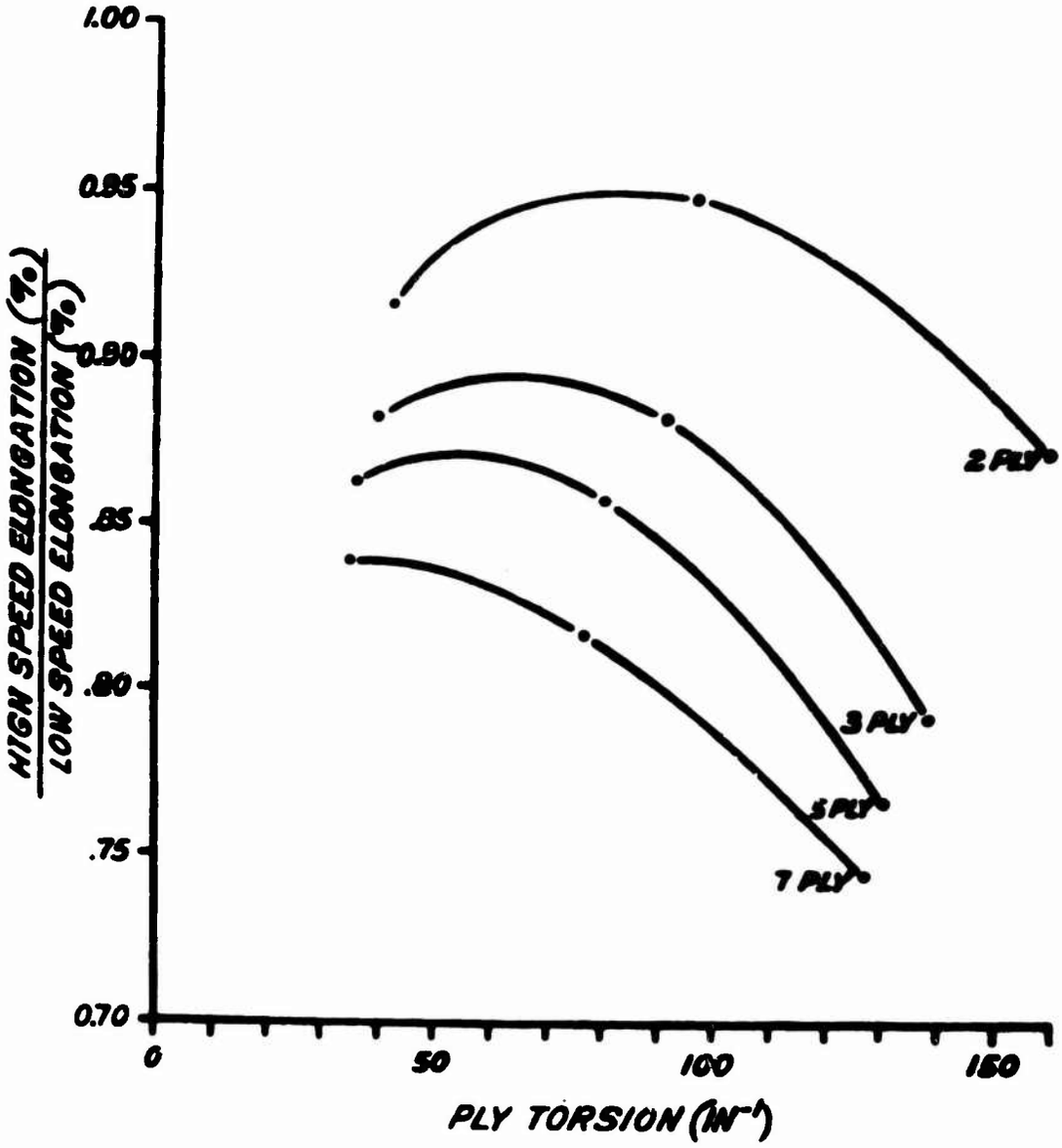

FIGURE 13 -ULTIMATE ELONGATION RATIO VS. PLY TORSION FOR NYLON 66 PLIED YARNS

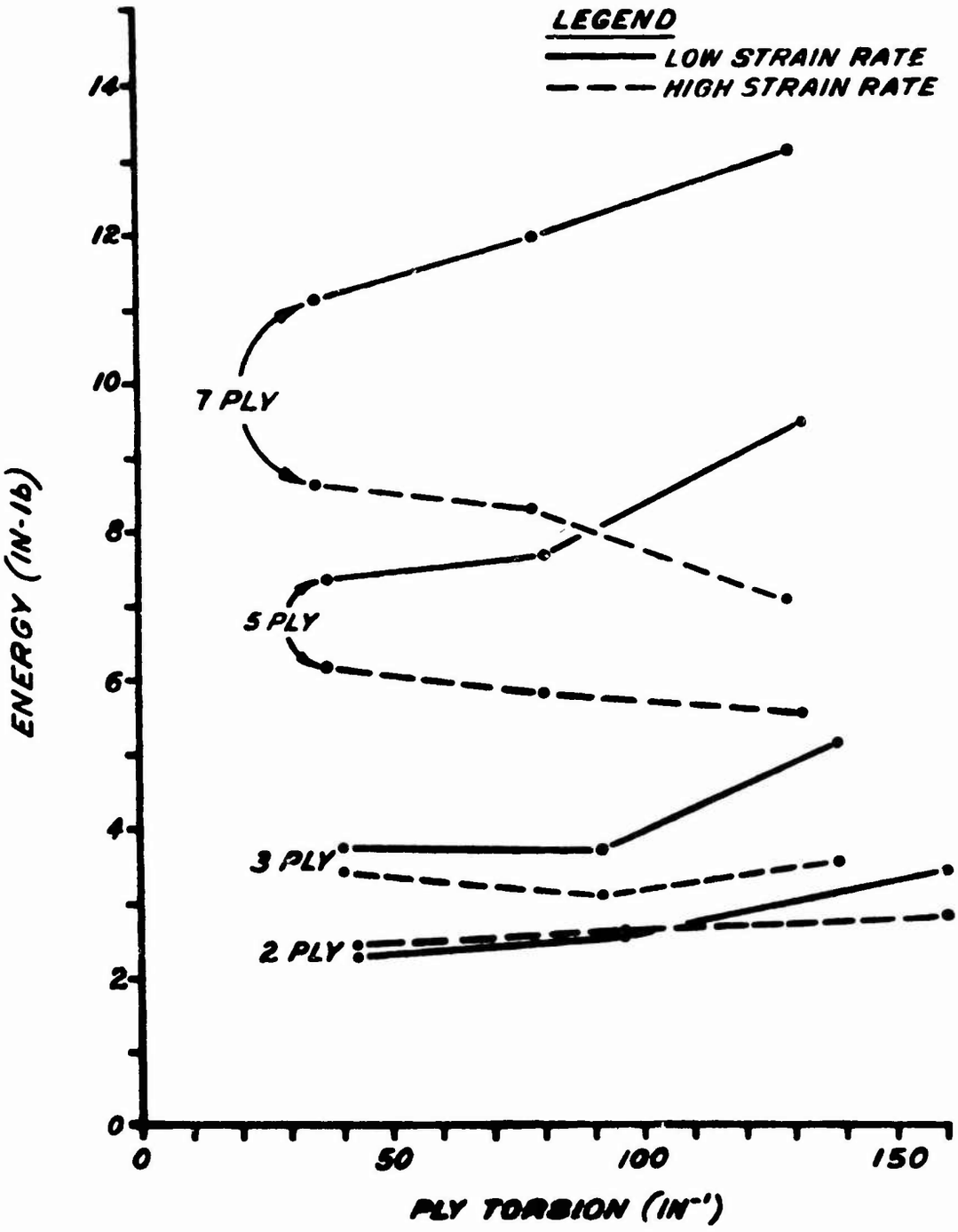

FIGURE 14 - WORK-TO-BREAK AT HIGH AND LOW STRAIN RATES VS. PLY TORSION FOR NYLON 66 PLIED YARNS

TABLE III

ENERGY EFFICIENCY OF NYLON YARNS

AT HIGH AND LOW STRAIN RATES

Energy Efficiency (%)

	Low Strain Rate			High Strain Rate		
	Actual Energy (in-lb)	Theoretical Energy (in-lb)	Efficiency (%)	Actual Energy (in-lb)	Theoretical Energy (in-lb)	Efficiency (%)
Single Ply	1.30			1.28		
3 ply 2 tpi	3.80	3.90	97.4	3.43	3.84	89.3
3 " 5 "	3.71	"	95.1	3.10	"	80.7
3 " 9 "	5.18	"	132.8	3.54	"	92.2
5 " 2 "	7.39	6.50	113.7	6.20	6.40	96.9
5 " 5 "	7.72	"	118.8	5.93	"	92.7
5 " 9 "	9.47	"	145.7	5.57	"	87.0
7 " 2 "	11.17	9.10	122.7	8.65	8.96	96.5
7 " 5 "	12.02	"	132.1	8.35	"	93.2
7 " 9 "	13.19	"	144.9	7.10	"	79.2

As ply is increased, it is seen that the high-speed values remain below the low-speed values with increasing differences between them.

Treatment of these data on an efficiency basis (Table III) shows that this increasing divergence is to a large extent due to the inability of the yarn to absorb energy at high strain rate to the same extent that it does at low strain rate. With increasing ply and twist, the energy-absorbing potential within the structure is increased because of the additional stretch capability. When the rate of loading is slow enough to allow for internal adjustments to take place, this increased potential is observable in the results. The energy efficiencies actually increase with structure to levels significantly greater than the theoretical maximums. However, when the same yarns are loaded at the rapid rate, they yield only a portion of their potential energy which is considerably less than their yield at low strain rate.

The high strain rate efficiencies also generally decrease with increasing ply and twist, which is the opposite of the results at low strain rate.

The relative energy capabilities at the two strain rates were compared as in the strength and elongation analyses. The ratios of high to low strain energy were plotted for each yarn at each torsional level (Figure 15). These ratios indicate the ability of the yarn to absorb energy under impact compared with its ability to absorb energy at low speed. This capability decreases with additional structural complexity. The seven-ply yarn under impact loading barely attains half of the low-speed energy yield at the high torsion level.

The trends noted in Figure 15 may be generalized by the expression:

$$y = a - bx \qquad (20)$$

where: $y = \dfrac{\text{high speed energy}}{\text{low speed energy}}$

$x = \psi_o^2$

With appropriate constants (see Appendix B, page 71), and without the curve for two-ply yarn, the applicable expressions become:

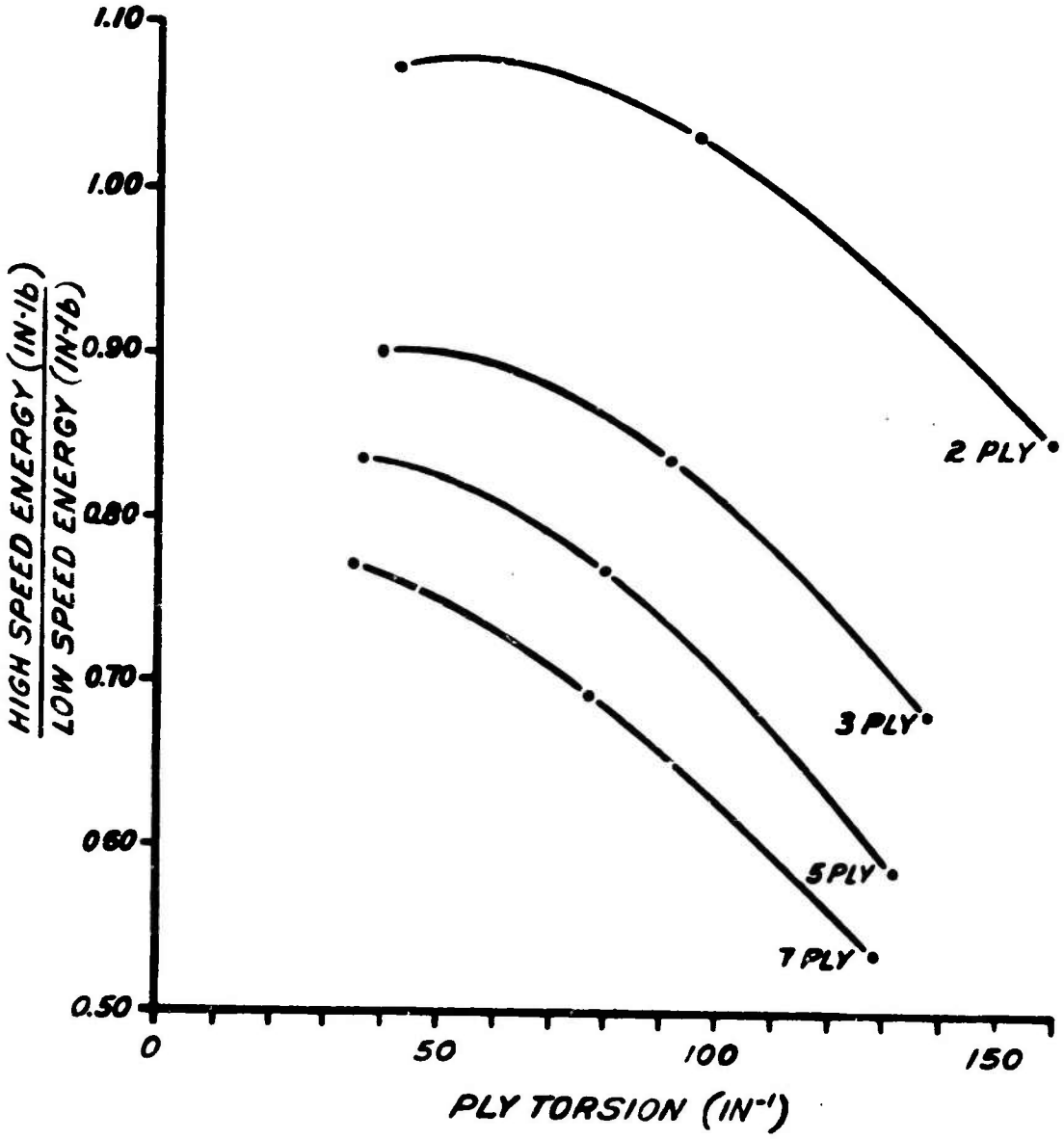

FIGURE 15 -WORK-TO-BREAK RATIO VS. PLY TORSION FOR NYLON 66 PLIED YARNS

$$3 \text{ ply} \quad WB_{HS} = WB_{LS} \left[.920 - 1.05 \times 10^{-5} (\psi_o^2)\right] \qquad (21)$$

$$5 \text{ ply} \quad WB_{HS} = WB_{LS} \left[.858 - 1.48 \times 10^{-5} (\psi_o^2)\right] \qquad (22)$$

$$7 \text{ ply} \quad WB_{HS} = WB_{LS} \left[.794 - 1.59 \times 10^{-5} (\psi_o^2)\right] \qquad (23)$$

where: WB_{HS} = Work-to-break at high strain rate
WB_{LS} = Work-to-break at low strain rate
ψ_o = ply torsion

(2) Stress-Strain Curves. The general behavioral characteristics for all plied yarns at both strain rates are characterized in Figure 16. The plots of specific stress vs. strain are arranged to show the comparative behavior for each yarn at the two strain rates and also the trends with ply and twist changes.

The ultimate properties observed serve to illustrate some of the trends previously discussed. The ultimate elongation at low speed increases with increases in twist and ply, while ultimate stress at high speed decreases.

The general shapes for all curves at low strain rate are similar, with the major differences being in the amount of extension near the rupture point.

The high strain rate curves, on the other hand, go through considerable changes in shape and inclination, from an almost linear behavior at two ply - two tpi to a more inclined and viscoelastic behavior at seven ply - nine tpi. Increases in twist bring about more pronounced dips in the post-yield regions, which are further amplified at the higher levels of ply, where the curves dip below those for low speed.

Since detailed analysis of the initial behavior was not warranted, the comparative stress-strain behavior of all the yarns was examined using ultimate properties through use of the secant modulus. Figure 17 shows that secant modulus decreases with ply and twist at both rates of loading with the values at high speed greater than those at low speed but decreasing more rapidly with torsion.

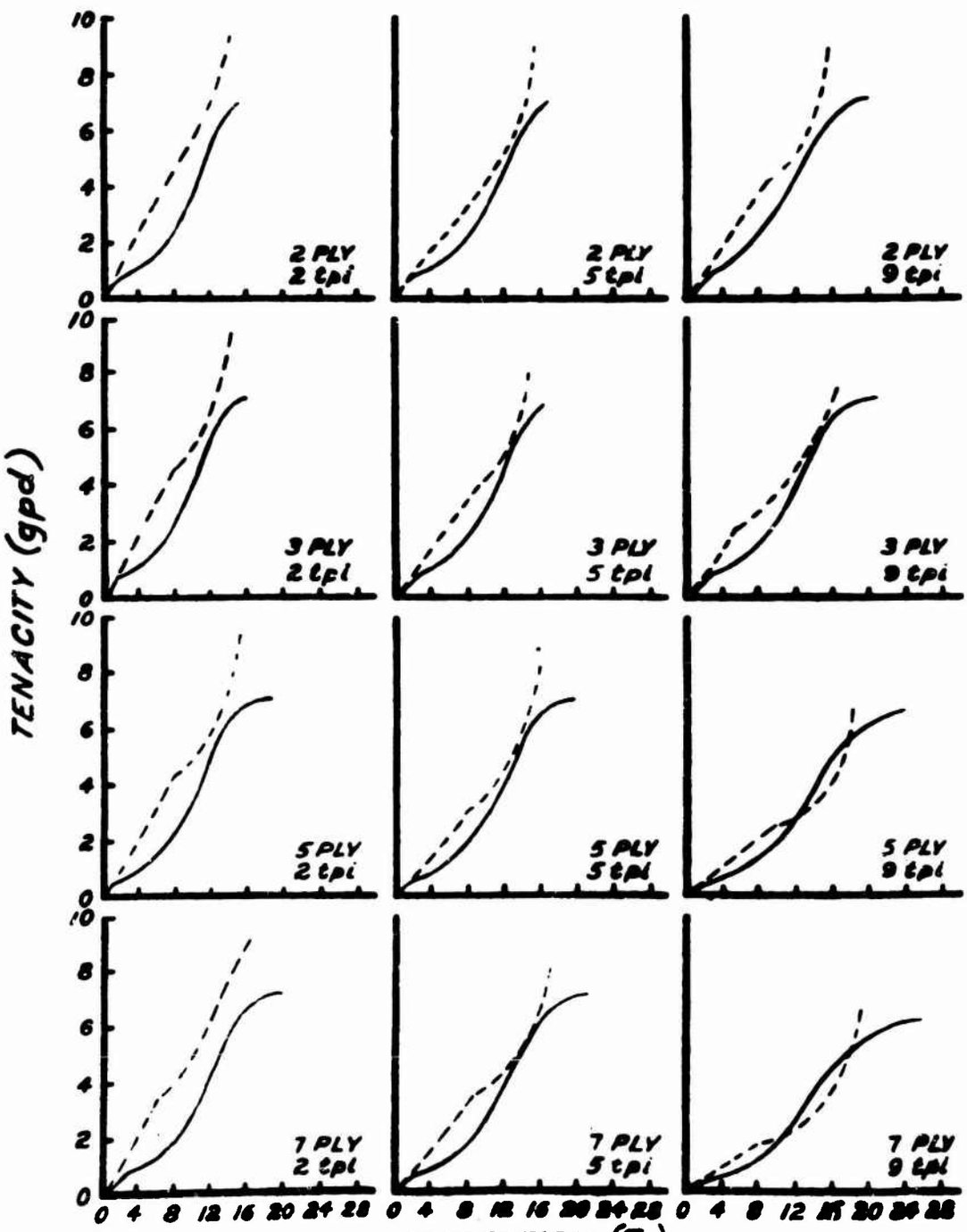

FIGURE 16 - STRESS-STRAIN CURVES FOR NYLON 66 PLIED YARNS
SOLID CURVES - LOW STRAIN RATE
DASHED CURVES - HIGH STRAIN RATE

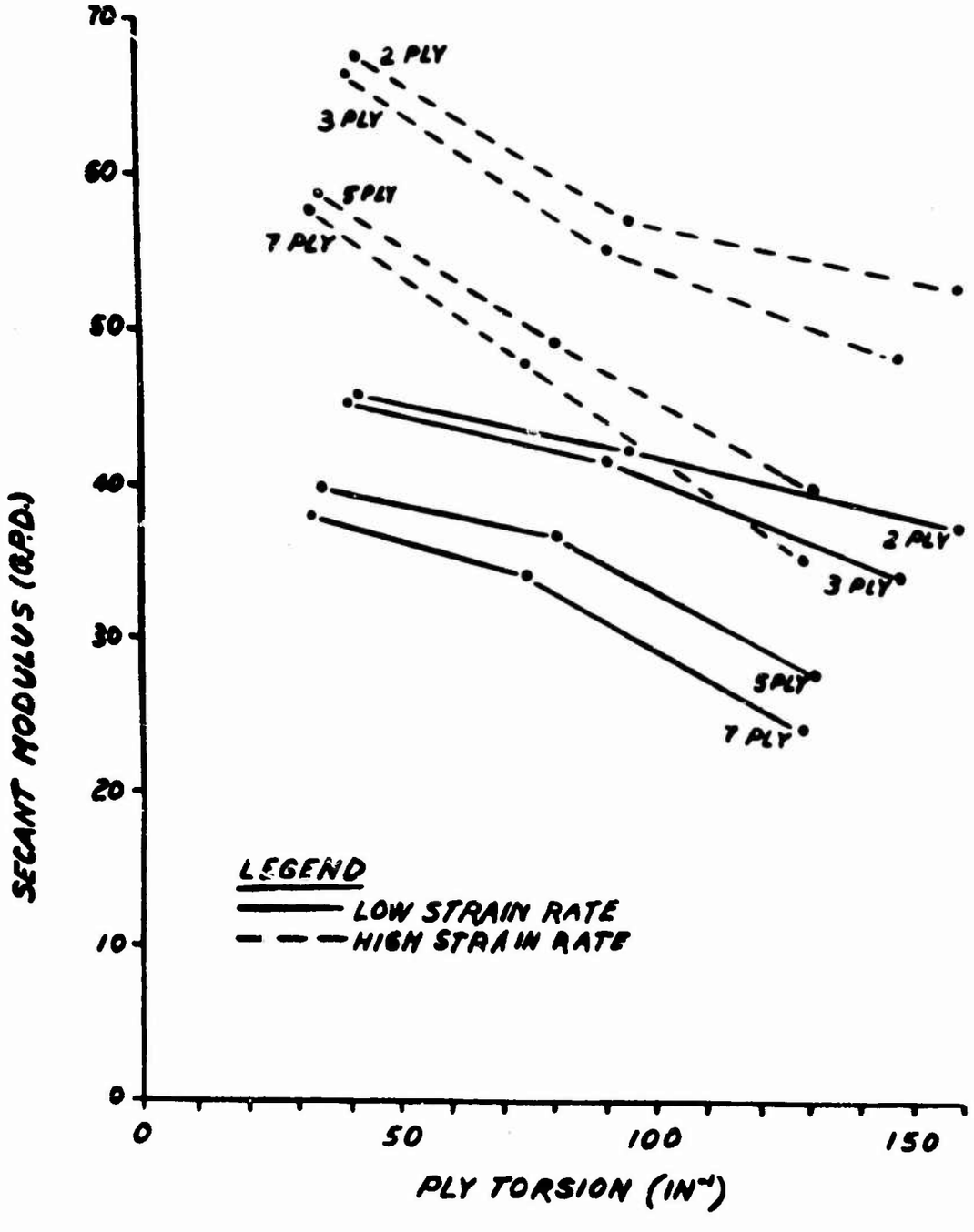

FIGURE 17- SECANT MODULUS VS. PLY TORSION FOR NYLON 66 PLIED YARNS AT HIGH & LOW STRAIN RATES

5. Conclusions

The results of this study led to the following conclusions, which are meant to apply only to the particular samples examined under the test conditions discussed. Further extrapolation of these conclusions beyond the conditions of fiber type, geometry, and strain rate specific to this study would be invalid.

a. Ply torsion for all plies examined increased as twist was increased from two to nine tpi. At every twist level the effect of increasing the number of plies was to bring about a decrease in torsion. Tortuosity of the ply axis about the principal axis of the yarn had a greater effect on total yarn torsion than did the torsion of each ply about its own axis.

b. Breaking strength losses due to increased translational complexities of plying and twisting occurred to a greater extent at strain rates of 288,000%/min than at 100%/min. The relative rate of loss with torsion is uniform and defined by equations (16), (17), (18) and (19). These relationships also provide a means for predicting, with a high degree of reliability, impact strength from data at conventional strain rates.

c. Ultimate elongation for all yarns was lower under impact loading than at the low strain rate. The potential stretch in the yarn was increased as ply and torsion of the structures increased, resulting in increases in elongation at both strain rates. However, a much greater portion of this potential was realized at the low strain rate.

d. Energy-absorbing capabilities were significantly different at the two strain rates. Work-to-break efficiency increased with structural complexity at the low strain rate but decreased at the high strain rate. These diverging trends culminated where barely 50 percent of the low-speed energy capacity could be achieved at high strain rate for the most complex structure. Relative energy characteristics were defined by equations (21), (22) and (23) which may also predict impact energy capacity from energy data at conventional strain rates.

e. Stress-strain curve shapes for the high strain rate tests were more susceptible to change over the range of structures examined. Secant modulus decreased with more complex structure at both strain rates, but more rapidly at high speed than at low.

The purpose of this study was to investigate structural effects which are believed to be beyond the influence of the basic polymeric behavior. Increases in geometric complexity complicate the force translation pattern through the system and hinder the internal readjustment process which takes place during axial loading.

It is felt that the differences noted in yarn response at the two strain rates reflect the levels of adjustment which could be achieved during the total loading times at each speed (9-15 sec, low speed; .003-.004 sec, high speed).

6. Recommendations

Textile items which are subjected to impact loadings during their use fall into many categories of structural design. Regardless of the final form of the item, however, yarns such as those evaluated in this study will almost always serve as the basic components of the item. A distinction is, therefore, made between textile end items and their structural components in considering future research.

A logical expansion of the present study at the component level would be toward yarns of increased complexity, i.e., more plies, higher twist, and ply-on-ply structures. It is felt that a minimum efficiency may be reached beyond which further structural complexity would have little effect.

Also at the yarn level, the effect of single-yarn denier and twist on ultimate ply yarn behavior may be worthy of investigation.

Considerable value would be derived from studies of structures with similar geometry but different fiber content. The relative efficiencies may uncover materials outstanding in the translation of impact forces which were not previously considered for such applications.

Though the evaluation of component yarns may provide a more complete understanding of the ultimate material behavior, there is no doubt that emphasis must be placed on the response of these components in the final configuration. The effect of various designs used in woven items, particularly webbings, presents a wide and important area for end-item research. Equally important are the effects of stitched splices and mechanical connectors on the impact efficiency of webbings.

Braids and cords also offer many possibilities for future work. The braid appears to be a highly inefficient structure under impact conditions; studying the effects of braid angle, bulk, yarn twist, and other factors may lead to an optimal braid design.

7. References

1. Woods, N. J., The Kinematics of Twist, J. Textile Inst., 24, T317 (1933).

2. Schwarz, E. R., Twist Structure of Plied Yarns, Textile Res. J., 20 (1950).

3. Treloar, L. R. G., The Stress-Strain Properties of Multi-Ply Cords, Part I. Theory, J. Textile Inst., 38, T477 (1965).

4. Riding, G., The Stress-Strain Properties of Multi-Ply Cords, Part II. Experimental, J. Textile Inst., 39, T489 (1965).

5. Tattersal, G. H., An Experimental Study of Yarn Geometry, J. Textile Inst., 49, T295 (1958).

6. Treloar, L. R. G., The Geometry of Multi-Ply Yarns, J. Textile Inst., 47, T348 (1956).

7. Leaderman, H., Impact Testing of Textiles, Textile Res. J., 13, No. 8, 21 (1943).

8. Schwarz, E. R., Samuel Slater Memorial Textile Laboratory, Textile Res. J., 15, 33 (1945).

9. Newman, S. B., and H. G. Wheeler, Impact Strength of Nylon and Sisal Ropes, J. Research NBS, 35, 417 (1945).

10. Parker, J. P. and C. S. Kemic, Energy Absorption in Tire Yarn During Impact Breaks, Fiber Society, Symposium on the Impact Properties of Textile Materials, New York, New York (6 September 1956).

11. Ballou, J. and J. A. Roething, High-Speed Tensile Testing of Fibers, Textile Res. J., 28, 631 (1958).

12. Lang, W. R., Ballistic Determination of Work of Rupture of Short Textile Fibers, J. Textile Inst., 42, T314 (1951).

13. Meredith, R., The Effect of Rate of Extension on The Tensile Behavior of Viscose and Acetate Rayons, Silk and Nylon, J. Textile Inst., 45, T30 (1954).

7. References (cont'd)

14. McCrackin, F. L., H. F. Schiefer, J. C. Smith, and W. K. Stone, Stress-Strain Relationships in Yarn Subjected to Rapid Impact Loading: 2. Breaking Velocities, Strain Energies, and Theory Neglecting Wave Propogation, Textile Res. J., 25, 529 (1955).

15. Chu, C. C., R. J. Coskren and H. M. Morgan, Investigation of the High-Speed Impact Behavior of Fibrous Materials, Part I: Design of Apparatus, WADD Technical Report 60-511, Wright Air Development Div., U. S. Air Force (Sept. 1960).

16. Supnik, R. H. and M. Silberberg, Properties of Foams and Laminates Under Shock Loading, Soc. Plastics Eng. J., 15, No. 1 (1959).

17. Smith, H. DeW., Textile Fibers: An Engineering Approach to Their Properties and Utilization, Proc. Amer. Soc. Testing Materials, 44, 543 (1944).

18. Smith, J. C., P. J. Shouse, J. M. Blandford and K. M. Towne, Stress-Strain Relationships in Yarns Subjected to Rapid Impact Loading. Part VII: Stress-Strain Curves and Breaking Energy Data For Textile Yarns, Textile Res. J., 31 (1961).

19. Lyons, W. J. and I. B. Prettyman, Use of the Ballistic Pendulum For Impact Testing of Tirecord, Textile Res. J., 23, 917 (1953).

20. Schwarz, E. R., Certain Aspects of Yarn Structure, Textile Res. J., 21, 125 (1951).

APPENDIX A

DEFINITIONS

Definitions

Torsion in A Single Strand

Figure 18 shows a rotating vector P, which represents a single strand component of a plied yarn. As this vector travels through the helical path PP', it rotates through 360 degrees about the Z axis. If N is equal to the twist per inch, then the distance travelled along the Z axis in one complete revolution is 1/N inch.

Torsion is defined as the rate of angular displacement of the vector with respect to the unit displacement along the Z axis or $d\phi/dz$. In this example (Figure 18), $d\phi/dz = 2\pi N$.

Tortuosity in A Single Strand

Figure 19 shows a section of the single component strand as it traverses a helical path about the Z axis. This strand is composed of individual filaments which spiral about the axis O of the strand. A set of coordinates is constructed at point X on one filament, where T is tangent to the filament at point X, and N is normal. If this set of axes were moved along the path of the filament with T remaining tangent at all times, then rotation of N about T would take place.

Tortuosity has been defined as the rate of this rotation and is described mathematically as:

$$\frac{\sin\alpha \cos\alpha}{\text{radius}}$$

where: α is the ply helix angle.

Ply Torsion

The total torsion for the plied yarn is defined as the sum of the torsion and tortuosity in the single strand.

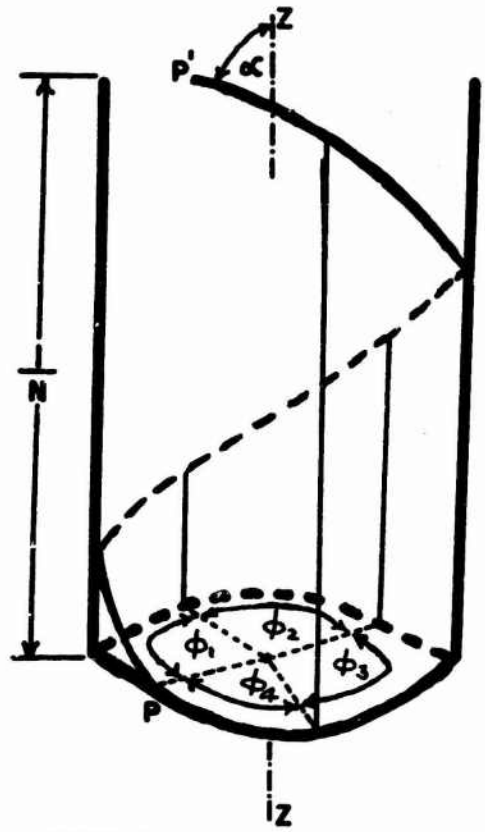

FIGURE 18-PATH OF SINGLE STRAND IN PLY YARN

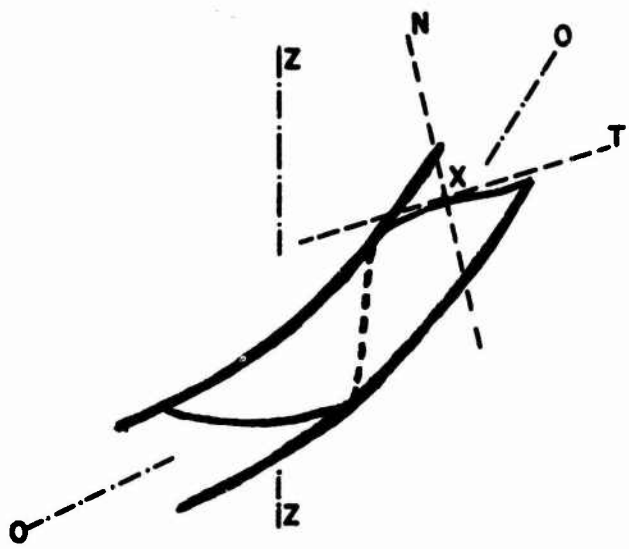

FIGURE 19-PATH OF FILAMENT IN SINGLE STRAND

APPENDIX B

TABLES IV--XII

TABLE IV

DATA FOR SINGLE PLY RETRACTION (l_s)

	"0" Twist Length, (in)	Intermediate Twist (total turns)	Length at Intermediate Twist, (in)	tpi	l_s
Run 1	25.05	0			
		91	25.00	3.64	.9980
		136	24.95	5.54	.9960
		168	24.90	6.75	.9940
		192	24.85	7.73	.9920
		218	24.80	8.79	.9900
		241	24.75	9.74	.9880
		261	24.70	10.57	.9860
Run 2	25.01	0			
		120	24.95	4.81	.9976
		158	24.90	6.35	.9956
		184	24.85	7.40	.9936
		208	24.80	8.39	.9916
		231	24.75	9.33	.9896
		251	24.70	10.16	.9876
Run 3	25.05	0			
		107	25.00	4.28	.9980
		148	24.95	5.93	.9960
		175	24.90	7.03	.9940
		202	24.85	8.13	.9920
		224	24.80	9.03	.9900
		247	24.75	9.98	.9880
		262	24.70	10.61	.9860
Run 4	25.01	0			
		80	25.00	3.20	.9996
		130	24.95	5.21	.9976
		168	24.90	6.75	.9956
		191	24.85	7.69	.9936
		213	24.80	8.59	.9916
		238	24.75	9.62	.9896
		257	24.70	10.40	.9876
Run 5	25.00	0			
		113	24.95	4.52	.9980
		146	24.90	5.86	.9960
		178	24.85	7.16	.9940
		204	24.80	8.23	.9920
		228	24.75	9.21	.9900
		256	24.70	10.36	.9880

TABLE V

DATA FOR PLY YARN RETRACTION (l_o)

Yarn Structure	(L) Twisted Ply Length (in)	(l_1) Untwisted Ply Length (in)			(l_1) Average (in)	Retraction (l_o)
2 ply - 2 tpi Z	20.00	20.04	20.02	20.02	20.0267	.9987
2 ply - 5 tpi Z	20.00	20.15	20.17	20.16	20.1600	.9921
2 ply - 9 tpi Z	20.00	20.42	20.46	20.43	20.4367	.9786
3 ply - 2 tpi Z	20.00	20.07	20.05	20.03	20.0500	.9975
3 ply - 5 tpi Z	20.00	20.19	20.20	20.19	20.1933	.9904
3 ply - 9 tpi Z	20.00	20.70	20.71	20.76	20.7233	.9651
5 ply - 2 tpi Z	20.00	20.07	20.07	20.06	20.0667	.9967
5 ply - 5 tpi Z	20.00	20.28	20.28	20.28	20.2800	.9880
5 ply - 9 tpi Z	20.00	21.28	21.24	21.29	21.2700	.9403
7 ply - 2 tpi Z	20.00	20.09	20.08	20.10	20.0900	.9955
7 ply - 5 tpi Z	20.00	20.50	20.47	20.42	20.4633	.9774
7 ply - 9 tpi Z	20.00	21.90	21.91	21.92	21.9100	.9128

TABLE VI

DATA FOR PLY HELIX ANGLES (DEGREES)

	2 ply - 2 tpi Z	2 ply - 5 tpi Z	2 ply - 9 tpi Z
	3	14	23
	4	14	24
	3	10	22
	3	11	23
	4	13	24
	4	11	20
	2	12	23
	4	14	20
	5	14	18
	3	12	22
Average	3.5	12.5	21.9
Std. Dev.	0.85	1.51	1.97
Std. Error	0.27	0.48	0.63

	3 ply - 2 tpi Z	3 ply - 5 tpi Z	3 ply - 9 tpi Z
	4	14	30
	4	13	20
	3	12	26
	5	15	26
	4	15	27
	6	13	25
	5	15	25
	5	12	25
	4	16	25
	5	14	24
Average	4.5	13.9	25.3
Std. Dev.	0.95	1.37	2.50
Std. Error	0.25	0.43	0.79

TABLE VI (cont'd)

DATA FOR PLY HELIX ANGLES (DEGREES)

	5 ply - 2 tpi Z	5 ply - 5 tpi Z	5 ply - 9 tpi Z
	5	21	33
	5	22	25
	9	19	33
	9	19	29
	9	21	29
	10	19	30
	5	21	29
	7	20	33
	8	18	26
	7	18	35
Average	7.4	19.8	30.2
Std. Dev.	1.90	1.40	3.26
Std. Error	0.60	0.44	1.06

	7 ply - 2 tpi Z	7 ply - 5 tpi Z	7 ply - 9 tpi Z
	10	20	32
	10	22	31
	8	20	35
	9	21	31
	9	22	31
	11	20	31
	9	26	31
	8	20	29
	10	23	30
	9	22	30
Average	9.3	21.6	31.1
Std. Dev.	0.85	1.90	1.60
Std. Error	0.27	0.44	0.40

TABLE VII

PLY AXIS RADIUS (a), AND DATA NECESSARY FOR SOLUTION OF EQUATION (5)

Ply/Twist (tpi Z)	Helix Angle (α)	Tan α	$dy = \tan \alpha / t$	$kd_y = d_h$	$a = d_h/2$
2-2Z	3.5	.06116	.009734	.004867	.002433
2-5Z	12.5	.22169	.014113	.007056	.003528
2-9Z	21.9	.40200	.014215	.007107	.003554
3-2Z	4.5	.07870	.012525	.006764	.003382
3-5Z	13.9	.24747	.015754	.008507	.004253
3-9Z	25.3	.47270	.016715	.009026	.004513
5-2Z	7.4	.12988	.020671	.013023	.006511
5-5Z	19.8	.36002	.022919	.014439	.007219
5-9Z	30.2	.58201	.020580	.012965	.006482
7-2Z	9.3	.16376	.026063	.017462	.008731
7-5Z	21.6	.39593	.025205	.016887	.008443
7-9Z	31.1	.60324	.021331	.014292	.007146

TABLE VIII

PLY YARN TORSION (Ψ_o) AND DATA NECESSARY FOR SOLUTION OF EQUATION (1)

Ply/Twist (tpi Z)	Ψ_s	l_s	l_o	a_o	$\sin\alpha$	$\cos\alpha$	Ψ_o
2-2Z	17.28	.9994	.9987	.002433	.06105	.99813	42.34
2-5Z	36.18	.9965	.9921	.003528	.21644	.97630	96.24
2-9Z	61.30	.9888	.9786	.003554	.37299	.92784	159.31
3-2Z	17.28	.9994	.9975	.003382	.07846	.99692	40.44
3-5Z	36.18	.9965	.9904	.004253	.24023	.97072	91.23
3-9Z	61.30	.9888	.9651	.004513	.42736	.90408	148.42
5-2Z	17.28	.9994	.9967	.006511	.12880	.99167	36.94
5-5Z	36.18	.9965	.9880	.007219	.33874	.94088	80.64
5-9Z	61.30	.9888	.9403	.006482	.50302	.86427	131.53
7-2Z	17.28	.9994	.9955	.008731	.16160	.98686	35.61
7-5Z	36.18	.9965	.9774	.008443	.36812	.92978	77.43
7-9Z	61.30	.9888	.9128	.007146	.51653	.85627	128.30

TABLE IX

YARN BREAKING STRENGTH MEASUREMENTS AT LOW AND HIGH STRAIN RATES

Ply/Twist (tpi Z)		Yarn Breaking Strength (lb) Individual Measurements					Avg
1/0.75	LS*	3.37	3.46	3.62	3.48	3.49	
		3.64	3.45	3.64	3.42	3.43	3.50
	HS*	4.86	4.86	4.43	4.86	4.43	
		4.29	4.57	4.43	4.29	4.29	4.53
2/2	LS	6.80	6.42	6.60	6.90	6.90	6.72
	HS	8.68	8.95	9.47	8.68	9.90	9.19
2/5	LS	6.72	6.89	6.70	6.89	6.83	6.81
	HS	8.18	8.70	8.96	8.57	8.18	8.52
2/9	LS	6.90	6.90	7.00	6.85	6.92	6.91
	HS	8.57	8.21	8.21	9.42	8.21	8.52
3/2	LS	10.18	10.33	10.15	10.08	10.33	10.21
	HS	14.06	12.50	13.75	12.19	14.06	13.31
3/5	LS	9.78	10.00	10.13	9.78	10.00	9.94
	HS	11.78	12.14	11.07	11.78	11.42	11.64
3/9	LS	10.20	10.25	10.40	10.25	10.33	10.29
	HS	11.71	11.71	11.84	12.10	11.32	11.74
5/2	LS	16.80	17.08	16.80	16.88	17.10	16.93
	HS	21.05	22.43	21.47	22.11	21.05	21.62
5/5	LS	16.75	17.00	16.60	17.03	16.93	16.86
	HS	19.99	21.42	16.42	17.85	21.78	19.49
5/9	LS	16.95	16.85	16.65	16.63	16.50	16.72
	HS	17.14	19.28	16.42	20.35	17.85	18.27
7/2	LS	23.65	24.40	24.65	24.15	23.75	24.12
	HS	28.56	30.35	33.21	31.06	29.63	30.56
7/5	LS	23.80	23.55	23.93	23.78	23.75	23.77
	HS	28.56	28.56	25.70	25.70	27.85	27.27
7/9	LS	22.75	22.55	22.28	22.45	22.55	22.52
	HS	25.71	23.57	23.93	24.29	23.57	24.21

*LS - Low Strain Rate - 100%/min
HS - High Strain Rate - 288,000%/min

TABLE X

YARN ELONGATION MEASUREMENTS AT LOW AND HIGH STRAIN RATES

Ply/Twist (tpi Z)		Ultimate Elongation (%) Individual Measurements					Avg
1/0.75	LS*	13.1	13.8	14.5	14.4	14.8	
		15.8	15.1	15.2	12.8	15.1	14.5
	HS*	13.2	14.0	14.8	13.0	14.8	
		14.0	13.0	14.0	12.0	14.0	13.7
2/2	LS	14.4	15.7	15.8	15.6	16.2	15.5
	HS	14.2	14.0	14.8	14.0	14.2	14.2
2/5	LS	16.0	17.0	15.7	16.7	17.6	16.6
	HS	16.4	16.0	16.4	15.4	14.4	15.7
2/9	LS	18.4	20.0	20.3	19.8	18.2	19.3
	HS	16.0	16.0	16.8	18.0	17.0	16.8
3/2	LS	15.6	16.6	15.4	15.6	17.0	16.0
	HS	15.6	13.0	14.2	14.0	13.8	14.1
3/5	LS	15.6	16.6	18.1	16.8	17.1	16.8
	HS	15.6	14.8	14.2	14.8	14.6	14.8
3/9	LS	20.7	19.5	21.2	21.2	20.6	20.6
	HS	16.0	17.4	15.8	16.2	16.2	16.3
5/2	LS	18.4	17.1	16.8	18.8	19.3	18.1
	HS	16.2	16.0	15.0	15.4	15.6	15.6
5/5	LS	17.4	19.9	17.8	19.8	19.7	19.0
	HS	14.4	16.4	16.8	17.6	16.2	16.3
5/9	LS	24.5	25.0	23.8	24.5	22.0	24.0
	HS	18.6	19.4	19.2	19.4	17.4	18.8
7/2	LS	18.2	20.2	20.2	19.3	17.7	19.1
	HS	15.5	16.0	16.6	16.1	15.8	16.0
7/5	LS	21.8	20.8	20.3	20.0	20.8	20.7
	HS	17.6	16.0	16.4	17.6	17.0	16.9
7/9	LS	26.5	26.4	25.0	24.7	24.8	25.5
	HS	18.2	21.6	18.4	18.0	19.0	19.0

*LS - Low Strain Rate - 100%/min
HS - High Strain Rate - 288,000%/min

TABLE XI

YARN WORK-TO-BREAK MEASUREMENTS
AT
LOW AND HIGH STRAIN RATES

Ply/Twist (tpi Z)		Work-to-Break (in-lb) Individual Measurements					Avg
1/0.75	LS*	1.01	1.13	1.27	1.24	1.24	
		1.50	1.36	1.43	1.44	1.36	1.30
	HS*	1.46	1.68	1.46	1.28	1.19	
		1.11	1.02	1.28	0.93	1.37	1.28
2/2	LS	2.37	1.89	2.18	2.40	2.51	2.27
	HS	2.49	2.43	2.53	2.29	2.49	2.44
2/5	LS	2.26	2.75	2.21	2.61	2.78	2.52
	HS	2.61	2.69	2.86	2.41	2.41	2.60
2/9	LS	3.12	3.55	3.73	3.43	3.16	3.40
	HS	2.54	2.77	2.65	3.54	2.88	2.88
3/2	LS	3.44	4.28	3.35	3.76	4.13	3.80
	HS	3.68	3.19	3.58	3.29	3.39	3.43
3/5	LS	3.26	3.62	4.26	3.53	3.89	3.71
	HS	3.54	2.88	2.88	3.10	3.10	3.10
3/9	LS	4.77	4.91	5.52	5.33	5.36	5.18
	HS	3.38	3.68	3.54	3.70	3.42	3.54
5/2	LS	7.52	6.32	6.61	7.94	8.57	7.39
	HS	6.32	6.55	5.96	6.05	6.11	6.20
5/5	LS	6.77	8.59	6.55	8.71	8.00	7.72
	HS	6.19	6.86	5.09	5.42	6.08	5.93
5/9	LS	7.74	11.19	9.82	10.12	8.47	9.47
	HS	5.20	5.64	4.87	6.30	5.86	5.57
7/2	LS	10.01	12.71	12.72	11.16	9.28	11.17
	HS	7.96	8.30	10.18	8.41	8.41	8.65
7/5	LS	13.53	11.87	11.40	11.10	12.20	12.02
	HS	9.30	7.36	8.02	8.59	8.49	8.35
7/9	LS	14.73	13.83	11.95	12.77	12.66	13.19
	HS	7.52	7.41	7.30	6.86	6.41	7.10

*LS - Low Strain Rate - 100%/min
HS - High Strain Rate - 288,000%/min

Data for Yarn Denier

Ply/Twist (tpi)	Weight (gms) /5 ft	Denier
2/2	0.0730	431
2/5	0.0729	431
2/9	0.0740	437
3/2	0.1088	643
3/5	0.1096	647
3/9	0.1131	668
5/2	0.1814	1071
5/5	0.1859	1098
5/9	0.1924	1136
7/2	0.2542	1501
7/5	0.2598	1534
7/9	0.2793	1649

Conversion from weight to denier:

$$\frac{\text{gms}}{5 \text{ ft}} \times \frac{3.28 \text{ ft}}{\text{meter}} \times 9000 \text{ meters} = \text{denier}$$

$$\text{gms} \times 5905.8 = \text{denier}$$

Determination of Constants a, b + c for Equation (14)

The trends noted in Figure 10 follow the general relationship:

$$y = ae^{-bx} + c$$

Evaluation of the constants a, b and c for each curve was accomplished by the following process:

Constant "c"

Select two points on the curve:

pt. 1 (x_1, y_1); pt. 2 (x_2, y_2)

Compute a third pt:

pt. 3 (x_3, y_3): where $x_3 = \frac{x_1 + x_2}{2}$ and $y_3 = \frac{y_1 + y_2}{2}$

Compute "c" by:

$$c = \frac{y_1 y_2 - y_3^2}{y_1 + y_2 - 2y_3}$$

The numerical values of "c" obtained for each curve were:

2 ply ;	0.910
3 ply ;	1.071
5 ply ;	1.058
7 ply ;	1.000

Constants "a" and "b"

Constants "a" and "b" are the intercept and slope of the straight line formed when Ln $(y - c)$ is plotted against x as in Figure 20.

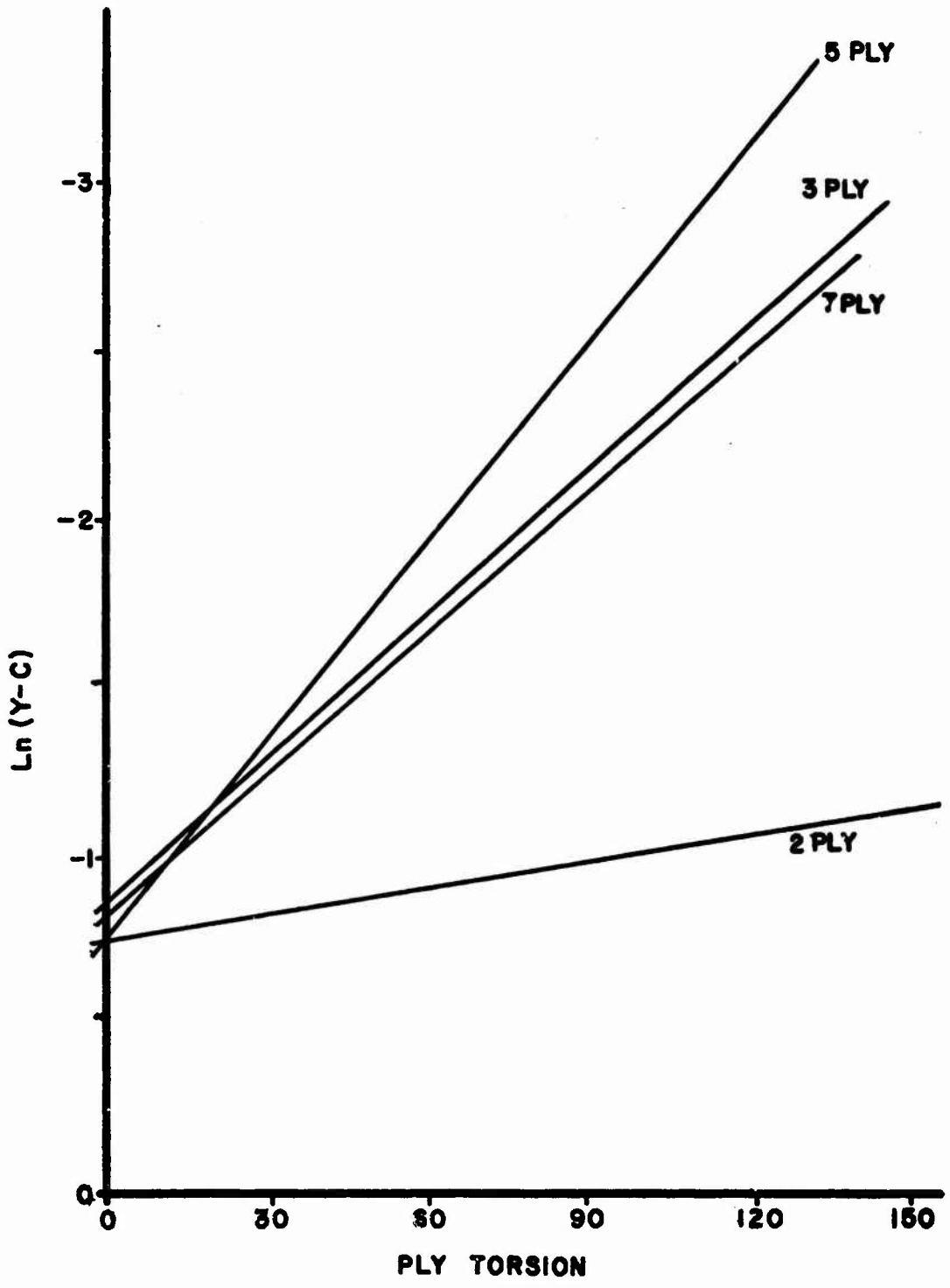

FIGURE 20 Ln(Y-C) vs TORSION FOR COMPUTATION OF CONSTANTS "a" AND "b"

Determination of Constants "a" and "b" for Equation (20)

The energy trends shown in Figure 15 are converted into straight line relationships when the abscissa values (ply torsion), are squared. From these plots (Figure 21) the numerical values of "a" and "b" for each ply group can be obtained from intercepts and slopes.

The results obtained were:

	Constant "a"	Constant "b"
3 ply	0.920	1.05×10^{-5}
5 ply	0.858	1.48×10^{-5}
7 ply	0.794	1.59×10^{-5}

Use of these constants in the general expression, equation (20) led to equations (21), (22) and (23).

The correlation coefficients for the straight line energy relationships (Figure 21) and also the strength relationships (Figure 20) are as follows:

Coefficient of Correlation (r)

	B.S. Data	Energy Data
2-ply	.903	
3-ply	.994	-1.004
5-ply	.999	-1.002
7-ply	.999	-1.002

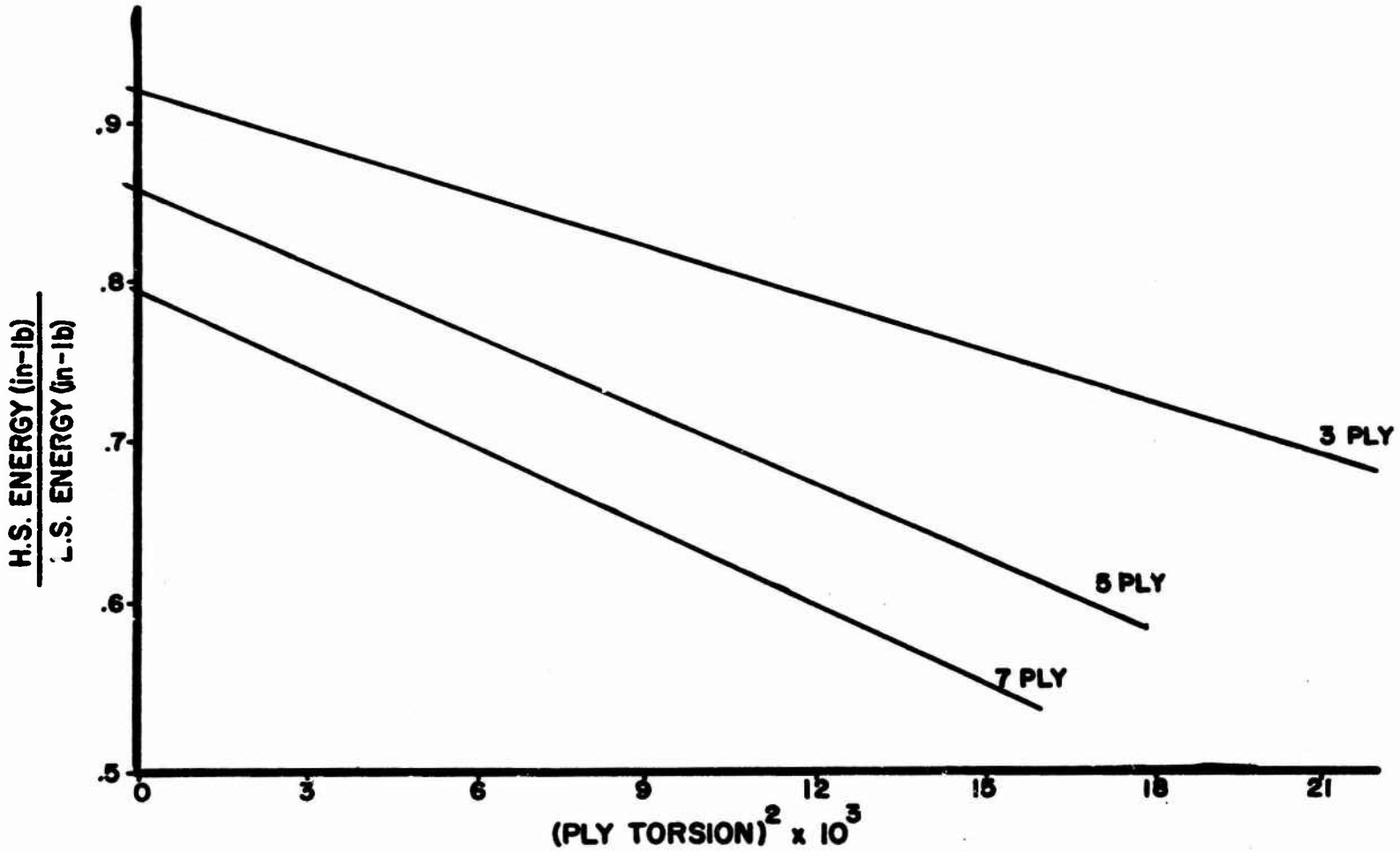

FIGURE 21-ENERGY RATIO vs TORSION FOR COMPUTATION OF CONSTANTS "a" AND "b"

Standard deviation values, not yet recorded, for strength, elongation and energy data (Appendix B, Tables IX, X, and XI) are listed in Table XII.

TABLE XII

STANDARD DEVIATIONS OF YARN BREAKING STRENGTH, ELONGATION AND WORK-TO-BREAK DATA (Appendix B, Tables IX, X and XI) (Percent)

Ply/Twist (tpi Z)		BS Data	Elongation Data	Work-to-Break Data
1/0.75	LS	.10	.96	.15
	HS	.24	.87	.23
2/2	LS	.21	.68	.24
	HS	.54	.33	.09
2/5	LS	.09	.76	.27
	HS	.34	.84	.19
2/9	LS	.05	.97	.26
	HS	.52	.83	.39
3/2	LS	.11	.71	.41
	HS	.90	.94	.20
3/5	LS	.15	.90	.38
	HS	.41	.51	.27
3/9	LS	.08	.69	.32
	HS	.28	.63	.14
5/2	LS	.15	1.08	.93
	HS	.63	.48	.24
5/5	LS	.18	1.21	1.01
	HS	2.31	1.17	.69
5/9	LS	.18	1.18	1.37
	HS	1.59	.84	.56
7/2	LS	.42	1.14	1.55
	HS	1.75	.41	.87
7/5	LS	.14	.68	.94
	HS	1.47	.72	.72
7/9	LS	.17	.89	1.09
	HS	.89	1.48	.46

Unclassified
Security Classification

DOCUMENT CONTROL DATA - R & D

(Security classification of title, body of abstract and indexing annotation must be entered when the overall report is classified)

1. ORIGINATING ACTIVITY (Corporate author)
U.S. Army Natick Laboratories
Natick, Massachusetts

2a. REPORT SECURITY CLASSIFICATION
Unclassified

2b. GROUP

3. REPORT TITLE
THE EFFECT OF STRAIN RATE AND PLY GEOMETRY ON THE STRESS-STRAIN PROPERTIES OF NYLON YARNS

4. DESCRIPTIVE NOTES (Type of report and inclusive dates)
Final Report, June 1969

5. AUTHOR(S) (First name, middle initial, last name)
Frank F. Figucia, Jr.

6. REPORT DATE	7a. TOTAL NO. OF PAGES	7b. NO. OF REFS
September 1969	72	20

8a. CONTRACT OR GRANT NO.	9a. ORIGINATOR'S REPORT NUMBER(S)
b. PROJECT NO. ITO--24401-A329	70-25-CE (C&PLSEL-165)
c.	9b. OTHER REPORT NO(S) (Any other numbers that may be assigned this report)
d.	

10. DISTRIBUTION STATEMENT
This document has been approved for public release and sale; its distribution is unlimited.

11. SUPPLEMENTARY NOTES	12. SPONSORING MILITARY ACTIVITY
	U.S. Army Natick Laboratories Natick, Massachusetts

13. ABSTRACT

The purpose of this study was to examine the changes that take place in the stress-strain behavior of plied yarns due to the differences in straining rates, and also the effects that yarn geometry has on these changes.

A series of 12 nylon plied yarns, representing a gradual buildup in geometric complexity, was examined. Ply structure was varied by twisting two, three, five and seven strands to various levels. A single untwisted strand was also used to provide reference data representative of yarn with relatively little translational complexity. Yarns were identified in terms of their ply torsion. This parameter, which provides a numerical description of the geometric orientation of the ply components, is calculated from their helix angle, diameter and retraction.

Tensile strength, elongation and work-to-break were measured for all samples at strain rates of 100 and 288,000%/min. These properties were then compared to geometric torsional levels, thus relating trends in physical yield to changes in structural complexity. They were also compared to the single strand reference data, providing an analysis of translational efficiency trends with structural changes.

Results showed that the capability to translate forces and energy through these yarns decreases with increases in geometric complexity under the impact loading condition. At standard quasi-static loading rates, however, strength translation remains fairly stable and energy translation increases with structure. Then the relative trends are diverging at the two test speeds. The use of low-speed data in the design of items for high strain rate use provides an overestimation of the actual end-use performance.

DD FORM 1 NOV 68 1473 REPLACES DD FORM 1473, 1 JAN 64, WHICH IS OBSOLETE FOR ARMY USE.

Unclassified
Security Classification

14. KEY WORDS	LINK A		LINK B		LINK C	
	ROLE	WT	ROLE	WT	ROLE	WT
Strain rate	6					
Yarns	6					
Geometry	6					
Plying	6					
Twisting	6					
Stress strain curves	7					
Nylon yarns	9					
Plied yarns	9					
Impact tests	4					

13. Abstract (cont'd)

Mathematical expressions were derived from which impact performance can be predicted from known information at conventional test speeds.